Landmine Detection Using Electromagnetic Spectral Signatures

By

Ali Ahmed

FALL-2020-MS-CS 00000330414 SEECS

Supervisor

Dr. Muhammad Imran Malik

Department of Electrical Engineering

School of Electrical Engineering Computer Sciences (SEECS)

National University of Sciences and Technology (NUST)

Islamabad, Pakistan

(September, 2021)

THESIS ACCEPTANCE CERTIFICATE

Certified that final copy of MS thesis entitled " Landmine Detection using Electromagnetic Spectral Signatures." written by ALI AHMED, (Registration No 00000330414), of SEECS has been vetted by the undersigned, found complete in all respects as per NUST Statutes/Regulations, is free of plagiarism, errors and mistakes and is accepted as partial fulfillment for award of MS/M Phil degree. It is further certified that necessary amendments as pointed out by GEC members of the scholar have also been incorporated in the said thesis.

Signature: _____

Name of Advisor: Dr. Muhammad Imran Malik

Date: _____25 May 2022_____
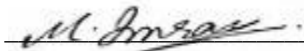
Signature (HOD): _____

Date: _____

Signature (Dean/Principal): _____

Date: _____

Approval

It is certified that the contents and form of the thesis entitled "Landmine Detection using Electromagnetic Spectral Signatures." submitted by ALI AHMED have been found satisfactory for the requirement of the degree

Advisor: Dr. Muhammad Imran Malik

Signature: _____

Date: _____25-May-2022_____

Committee Member 1: Dr. Moazzam Fraz

Signature: _____

Date: _____25-May-2022_____

Committee Member 2: Dr. Ali Tahir

Signature: _____

Date: _____25 May 2022_____

CERTIFICATE

Certified that the Scrutinizing Committee has reviewed the final documentation of Mr./Mrs/Miss: **Ali Ahmed Khan** Registration No: **330414** Student of: **MSCS, SEECS** Thesis title: **Landmine Detection using Electromagnetic Spectral Signatures**. Has been found satisfactory as per NUST's standard format for Master Thesis.

President

Nasir Mahmood

Assistant Professor

28 May, 2022

Dedication

I dedicate this effort to my mother who always supported me and pushed me in any way possible to become what I am today. Her sacrifices seeded my success. I also thank my advisor sincerely who always supported me and pushed me throughout this journey.

Certificate of Originality

It is certified that MS Thesis Titled: "Landmine Detection using Electromagnetic Spectral Signatures." By Ali Ahmed has been examined by us. We undertake the follows:

a. Thesis has significant new work/knowledge as compared already published or are under consideration to be published elsewhere. No sentence, equation, diagram, table, paragraph or section has been copied verbatim from previous work unless it is placed under quotation marks and duly referenced.

b. The work presented is original and own work of the author (i.e. there is no plagiarism). No ideas, processes, results or words of others have been presented as Author own work.

c. There is no fabrication of data or results which have been compiled/analyzed.

d. There is no falsification by manipulating research materials, equipment or processes, or changing or omitting data or results such that the research is not accurately represented in the research record.

e. The thesis has been checked using TURNITIN (copy of originality report attached) and found within limits as per HEC plagiarism Policy and instructions issued from time to time.

Student Name: ALI AHMED

Student Signature: _____

Acknowledgement

I am thankful to my Creator Allah Subhana-Watala to have guided me throughout this work at every step. Indeed I could have done nothing without His priceless help and guidance. Whosoever helped me throughout the course of my thesis, whether my parents or any other individual was His will, so indeed none be worthy of praise but Him.

I am thankful to my mother who continued to support me throughout in every department of my life. I would also thank my aunt, without her support I would not have been able to attend the institution or reach where I am today.

I would also like to express special thanks to my supervisor Dr. Muhammad Imran Malik for his help throughout my thesis. Each time I got stuck in something, he came up with the solution. Without his help I wouldn't have been able to complete my thesis. I appreciate his patience and guidance throughout the whole thesis.

I would also like to thank Dr. Moazzam Fraz and Dr. Ali Tahir for being on my thesis guidance and evaluation committee and express my special thanks to them for their help.

Finally, I would like to express my gratitude to all the individuals who have rendered valuable assistance to my study.

Ali Ahmed

Table of Contents

List of Abbreviation and Symbols

1. **ERW**   Explosive remnants of war
2. UXO   Unexploded Explosive Ordinance
3. PTSD   Post-traumatic stress disorder
4. AP   Anti-personnel
5. AT   Anti-Tank
6. GPR   Ground Penetrating Radar
7. IR   Infra-red
8. EM   Electromagnetic
9. NQR   Nuclear Resonance Response
10. R&D   Research and Design
11. VNIR   Visible & Near Infrared
12. SWIR   Short Wave Infrared
13. MWIR   Medium Wave Infrared
14. LWIR   Long Wave Infrared
15. HE   Histogram Equalization
16. PCA   Principle Component Analysis
17. SVM   Support Vector Machines
18. ML   Machine Learning

List of Figures

Abstract

The aim of this thesis was to test and report the applicability of ESS or electromagnetic spectral signature based imaging techniques to detect and identify landmines in both surface deployment and buried deployment. Traditional techniques such as metal detector based listeners while being low cost are being phased out due to the nature of modern constructed landmines. Small IR cameras are cheap and available thanks to the Chinese imports and can be mounted to a small drone to scan vast fields of land in a short period of time. In relative physics, every surface and material has its own electromagnetic signature according to which it reacts with spectral radiation such as light. This results in unique emittance and absorption responses and even color. By applying changing electromagnetic radiation over an object, we can acquire an entire spectral curve which can then be used to decide if a certain object is present at a specific pixel location in the image. For this project, we acquired data on electromagnetic spectral responses for American landmines primarily the claymore and the BLU-43 (butterfly) across various terrains and conditions. A spectral dictionary and bands were defined and the region around 750nm to 1100nm was selected which coincided with LWIR and MWIR bands. The datasets acquired had to undergo several pre-processing techniques and corrections. We rigorously tested all the processes involved from atmospheric corrections to classification, finding out how to reduce computation time to attain real time detection. There were several tradeoffs between detection performance and computing time. We studied several noise factors over the signatures such as wind and rain. We then tested multiple architectures of supervised detection algorithms with our preference to use simpler lighter classifiers to keep computation cost and time minimal.

Chapter 1

1.1 Introduction

Explosive Ordinance such as Landmines continue to remain a threat against societal development and return to normalcy even after ceasefires are agreed. The death and destruction do not stop with the end of the conflict but continues to rage on with unexploded ordinance such as cluster munition, landmines and improved explosives. These weapons do not know that the war has ended and remain active decades after being planted hurting innocent people in their daily lives.

In Recent Statistics [1], More than 70% of the causalities from landmines are children having no connection to the wars and their causes. Thus such blind and indiscriminate weapons should urgently be banned. The cause to ban their uses has gained traction lately and there are several international campaigns to ban cluster munitions, landmines and other indiscriminate ordinance with several signatory countries [2]. That said, no one can control a wartime situation and landmines have seen usage in recent Middle Eastern conflicts such as in Libya, Syria, Afghanistan and Iraq. This will be a future catastrophe and thus we should be working to find efficient algorithms and techniques that will be both fast and reliable.

There are different approaches to detect landmines, each of these approaches have their own pros and cons. The earliest and most widely adopted technique is the use of specialized metal detectors which employ the use of electrical induction phenomena. These detectors are able to detect objects containing metals under soil. This approach while being fast and cheap has several considerations, firstly it detects any and all kinds of metals so any inert metal junk may cause unacceptably high false alarms, secondly modern landmines are manufactured using plastic and contain very little metals so they will be incredibly hard to detect.

Our thesis addresses the problem with a novel employment of hyper spectral Imaging/Spectroscopy using Object Signatures. This approach uses the ability of modern IR imaging systems to measure for each pixel, portions of reflected light in 100s of wavelengths. We thus obtain a 2D hyper image consisting of 2 spatial dimensions but also spectral information for each pixel. Hyper spectral Imaging is already well used in contemporary remote sensing for agriculture, monitoring and surveillance, mapping and so on.

When light hits any object in its path, it can either be absorbed or reflected. Whatever portion is reflected is the factor of the size of the object's molecules, intermolecular distances and wavelength of the light. Thus a material composing several components can each reflect radiation of various lambdas (wavelength) differently. This signatory behavior is our key to identify a material remotely. In our example, we can utilize our hyper spectral imaging information to detect unexploded munition without physical presence on the ground.

Even within Hyper spectral Imaging there are several techniques to detect a target, many of these are supervised meaning that the spectral data is known beforehand. Others yet consist of

unsupervised search for any object in a location spectrally different from its surroundings. This detection approach does not require any advanced knowledge of target spectrum but plagues from unnecessarily high false alarms as we well discuss in coming chapters. The high rate is for most part due to rare phenomena such as noise in the image begin sufficiently different from its surroundings to be labelled a target.

For our MS Thesis, we studied several scenarios with different detection approaches of both supervised/unsupervised, we cater for several pre-processing techniques in the images such as feature selection, reduction of dimensionality and so on. Even if we know the reflectance spectrums of landmines and other target ordinance, their detection will not be so simple, take for example the following cases:

- Noisy Image itself, any processing cannot combat noisy pixels or mistakes from the Imaging Equipment.
- Spatial Resolution, Low resolution will make detection reflectance for a pixel overlap or mix with other spectra, this may in rare events cause a false alarm.
- Variability, spectra calculated in lab and field will be different due to background conditions, take into account temperature, humidity, illumination, etc.

In the next part, we define the unexploded ordinance problem further and explore existing methods currently employed to combat it. We will introduce the subject of hyper spectral Images with SOTA techniques and tools available at our disposal.

1.2   Unexploded Ordinance Problem

This part introduces the problem with unexploded explosives, the issues they cause, their legacy and actions against them. We analyze the explosives themselves, their types and their workings and several international programs to detect them. It is necessary to begin at the heart of this project, the workings of mines. We will concisely define their types and working, operating zones, ranges, blast radius, and so on, by adequately describing the main types of ordinance we are detecting. Some of the information we show was published at [3].

Many combat zones suffer as there are millions of pieces of unexploded ordinance within civilian territories. These devices have extremely long shelf lives and will deal tremendous economic losses and injuries decades after the conflict has ended. It is thus a need of the day to call of reliable inspection systems. This issue adversely affects the development of the regions such as killing of innocent civilians and causing horrific injuries leading to amputation of limbs or deaths [4, 5, 6, 7]. It also reduces the area that can be cultivated for agriculture [8, 9, 10, 11]. As an example, in Cambodia, there are more than 40,000 amputees due to landmines [4, 7] many of which were planted during the Vietnam Conflict. Most victims will die due to excessive bleeding long before they can be transported to a nearby medical facility [7]. Thus such ordinance will prevent valuable income in terms of foreign exchange that can be earned through tourists.

Many issues are faced when trying to remove landmines, military organizations that planted the ordinance may lose information about types of explosives used or maps on areas they were originally buried. Indeed, locations of landmines may change themselves due to climate and physical phenomena, then come the many types of unexploded ordinance and the huge cost of removal of the ordinance once it has been located. Landmine's sensitivity to explode may change with time or atmosphere so that's another danger.

Landmines are victim activated pieces of ordinance and due to their nature indiscriminate. Explosive remnants of war (ERW) are responsible for maiming and killing at least 4,000 people each year [5] with the overwhelming majority being civilians (80% for 2015) in which children were recording at 39%. Between 2000 to 2012 more than 1000 demining operatives have been victims while trying to diffuse an ERW [12].
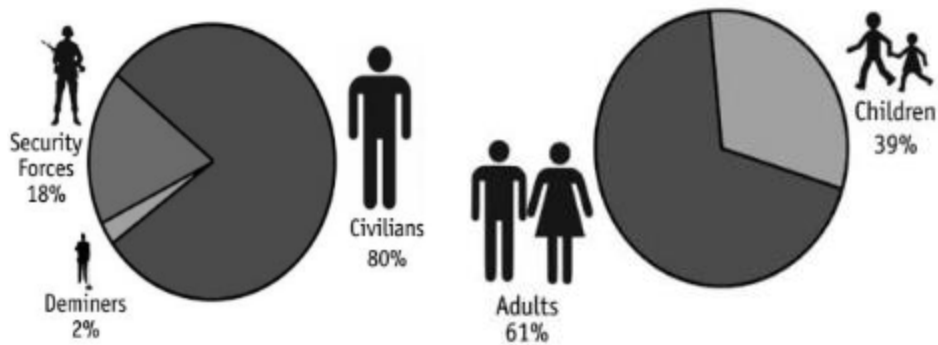
Figure 1: ERW causality by civilian/military and age.

The reason we showed the year 2014-15 is because this year had record losses since 2006 with the US withdrawal from Iraq and ISIS problem. The records of the losses come from the Monitor.org [3].

When landmines detonate, the impact decreases as we move away from the fallout core (mine itself). The shock wave from the explosion is at its peak in the beginning and loses momentum and energy to the atmosphere and incoming objects. Thus, a smaller mine with less explosive will have more killing power in closer contact than a larger one further, e.g. a mine under a small van or an IED in a packed bazaar. There is also a large assortment and ambiguity in the scope of wounds from IEDs and ERWs due to the touchy nature. These UXO (unexploded Explosive Ordinance) have two effects. First, is the personal impact to the victim and their family and secondly, economic and political impact to the nation as a whole. The first impact is the affected capacity of the victim and his family to acquire wages and afford economic wellbeing for their family. More than just physical wounds, the mental harm such as trauma, PTSD will adversely affect their employment opportunities and marriage prospects (especially in the case of an injured female) this is more serious for Middle Eastern Islamic society where mental disorders are taboo and victims are often outcast. This impact is not just limited to their immediate family,

the second impact e.g. treating of the horrific wounds will deplete medical resources of the organizations of the country, which are scarce in developing countries such as Pakistan. Unavoidably, such wounds will typically require 3-4 operations to amputate, stitch wounds, remove debris, etc. Every loss regrettably will further require prosthetics and/or wheelchairs to give the victim another chance for movement. Prosthetics once again will require concentrated therapy and plastic surgery to best utilize counterfeit limbs. Moreover the victim will require several years of therapy and state monetary support during the recovery progress. There are also political losses as the country is branded unsafe for travel, visa bans are issued, along with dozens of other considerations.

1.3 International Mine Action Standard

The United Nations put forward a first proposal for IMAS in March of 1997. An International Standard was formally accepted in 2000. This led to many countries updating their clearing procedures, training of staff, risk education as well as decommissioning techniques. This Standard was supported by GICHD or the Geneva International Centre of Humanitarian Demining. These set of standards was constantly updated to account for any new scientific or organizational developments. The primary goal being a consistent and standardized way to safely and efficiently identify and clear landmines.

The standards may apply in three key areas. To begin with, it is regarded as a template for any organization tasked with demining to ensure it adheres to contemporary standards and professional conduct. Next, it provides a set of standards around which a country can draw its own evaluation standards. Lastly, it defines the demining process as a set of pre-defined stages and advises what kind of equipment to commission at each stage. The stages are given below:

1. Identify the mined area

2. Determine the borders of contaminated zone within the area

3. Confirm the location and presence of individual landmines

4. Remove the suspected device

5. Confirm that the area is safe for civilians

Finally there is a notable difference between humanitarian demining (HU-DEM) and military clearing procedures. HU-DEM aims to identify, remove and completely neutralize any and all landmines planted in a civilian area while a military clearance procedure usually requires a rapidly cleared path to navigate a minefield during a conflict.

Before a demining operation can commence, its clearance specifications must be finalized. Following IMAS clearance specifications usually a standard one looks as follows. Firstly a technical survey and up to date geographical information must be collected. One of the most important

detail being the specified operating depth of this clearance operation. This depth is selected according to the type of landmine suspected to be deployed and other hazards associated. Normally a 100mm to 150mm is the maximum depth after which the explosive is deemed too deep to cause a hazard, this is also the effective depth ceiling most metal detectors can optimally function around. The use of mine detection device and technique will vary according to the area the landmine is deployed inside. IMAS tabulates and standardizes them into 12 different scenarios that can play out. The table below describes the scenarios and their characteristics.

Categories	Characteristics
Grassland	Open (flat or rolling) land
Woodland	Heavily wooded land
Hillside	Open hillside
Routes	Unsurfaced roads and tracks, including 10 m on each side
Infrastructure	Surfaced roads and railway tracks, including 10 m on each side
Urban	Large town or city
Village	Rural population centre
Mountain	Steep and high altitude
Desert	Very dry, sandy environment
Paddy field	Land allocated for growing of rice
Semi-arid savannah	Dry, open and flat, little vegetation
Bush	Significant vegetation and possible rock formations

Figure 2: The 12 standard scenarios and their characteristics.

1.4   Types of Landmines

UXO in general and landmines in particular can be broadly generalized into two roles, Anti-personnel (AP) designed for being detonated by people/soldiers and Anti-Material or Anti-Tank (AT) which are designed for destroying military vehicles and tanks [13]. As a military saying goes, while a bullet may have your name on it, AT mines are addressed "To whom it may concern" and AP mines are a general public announcement.

Anti-Material Ordinance is supposed to be detonated by motor vehicles like trucks and tanks that are large in size. These mines are commonly bigger than an adult's shoe, due to their size they can be quite heavy, usually at least 5 kgs. Such devices may contain a lot of explosive material

required to obliterate a heavy vehicle that runs over them and consequently due to the large blast radius also usually kill any unfortunate nearby people and vehicles. These devices are usually laid along where enemy vehicles will probably travel such as tracks, roads and bridges.

Anti-Personnel or AP Ordinance is are far easier to detonate and its objective is simply to injure people. It has a lot less explosive material but contain usually a lot of fragmentation material that will scatter everywhere during the detonation, e.g. 100s of steel balls that will spread around with a bullet's speed when the explosives underneath detonate. These devices are much smaller and lighter and could be as small as a pack of cigarettes with weights as small as a mere 50g. AP mines can come in all shapes and sizes being manufactures from a wide selection of materials.

Even though AP mines may kill people, their primary role is designed around causing severe wounding as an injured soldier will require medical and physical assistance and this will deplete enemy's morale and resources as well as delay them. Almost all paramilitary organizations use them against government forces because injured soldiers raise political costs, this was a major weapon in the hands of the Taliban and instrumental in the outcome for Afghanistan. These devices can be paid everywhere and can even be camouflaged as a small stone or a toy for children. They can be detonated in almost all creative ways such as being stepped on, by a physical wire or calling through phone and even by simply shaking the mine. AP mines are even designed be detonated if an object that was placed over them is taken away [14].

type	AP landmine	AT landmine
weight	Light(100g-4Kg)	Heavy(6Kg-11Kg)
size	6-20cm	20-50cm
target	Human	Vehicle
Case material	Plastic,metal,wood	Plastic,metal
Operating pressure	5Kg	120Kg

Figure 3: Statistics of AP and AT mines

Of more interest to us are AP Mines and they can further be categorized into two main types. Blast/Explosive Mines & Fragmentation Mines.

Blast/Explosive mines can usually be buried quite close to the ground surface and pressure triggered. As it is activated, the mine's charge or payload detonates creating a shock wave. This shockwave is usually extremely hot gases travelling at high speeds. Thus these mines are also called HEAT mines or scatterable mines, a famous example is the Willie Pete grenade [15].

Fragmentation devices release fast moving fragments in addition to a shock wave upon detonation. The fragments will travel in all directions but may be made to travel in one specific direction causing injuries to anyone up to 200m from the fallout "eye" and are fatal within 100m. The fragments are usually made out of glass or metal [16].

AT mines are designed to destroy or at least immobilize moving vehicles and thus all AT mines are blast mines as there is no need for a fragmentation charge to destroy a tank's tracks or chassis. Most military forces employ landmines to protect their military installation from intrusion. When a base is constructed, it may be attacked from all sides and thus landmines may limit the infiltration from a tactical zone and so defense can be more focused on another side. Mines may also be employed close to the artillery at the back of the military unit to avoid a flanking attack.

Thus mines by their design and nature will inevitably lead to civilian causalities. Their neutralization and removal requires professional experience and yet continue to be a costly and hazardous process as design of the mine was such to make their detection as difficult a task as possible, often employing camouflage. Moreover the problem has scaled in modern times as newer mines are manufactured in plastic and contain trace amounts of metals if at all. Furthermore SOTA mines may contain electronic equipment which may trigger the mine if removed such as a failsafe detonation.

1.5 Contemporary Detection Techniques

This section outlines the most employed contemporary UXO and landmine detection techniques. The goal of this section to explore the most widely employed techniques together with their advantages and drawbacks and finally compare their performance to the hyper spectral Imaging Techniques.

Most commonly employed methods for mine detection follow pretty much the same principles as detectors employed during WW2 and required direct involvement of skilled operators. In many ways a typical detection kit will mostly still resemble something out of cold war era as it was 70 years ago, a modified metal detector and a rod for prodding.

While many techniques exist, each has its own pros and cons, depending on conditions, types of mines to be detected, the soil and the explosive material in the mines. We now go through some contemporary techniques currently in use, the section aims not to define the electronics or physics behind them but merely to give a reader information about them stating their limitations and pros, thus the reader will appreciate the advantages hyper spectral imaging brings over them.

In a more generalized manner, any detection technique will have three modules or phases, a sensing module to capture the landmine signal, an image/signal processing module to process the data e.g. for noise removal or arranging, etc. and finally a decision module to decide whether the landmine is present in the data. The construction of the modules can take advantage of any

spectral or physical phenomena such as acoustic waves, electromagnetic waves, nuclear radiation or mechanical systems.

Electromagnetic Induction

An operator holds the induction coil detector close to the soil sweeping it slowly left to right around the area. Current through the first "transmitter" coil will induce time varying primary magnetic field in metallic clutter underneath the soil. This field will then induce eddy currents in the buried metallic clutter. The eddy currents will induce weaker, counter magnetic fields in the clutter and a second highly sensitive "receiver" coil will detect changes in its voltage induced by any counter magnetic fields close to it. These changes are then translated from electrical signals to audible tones [17].
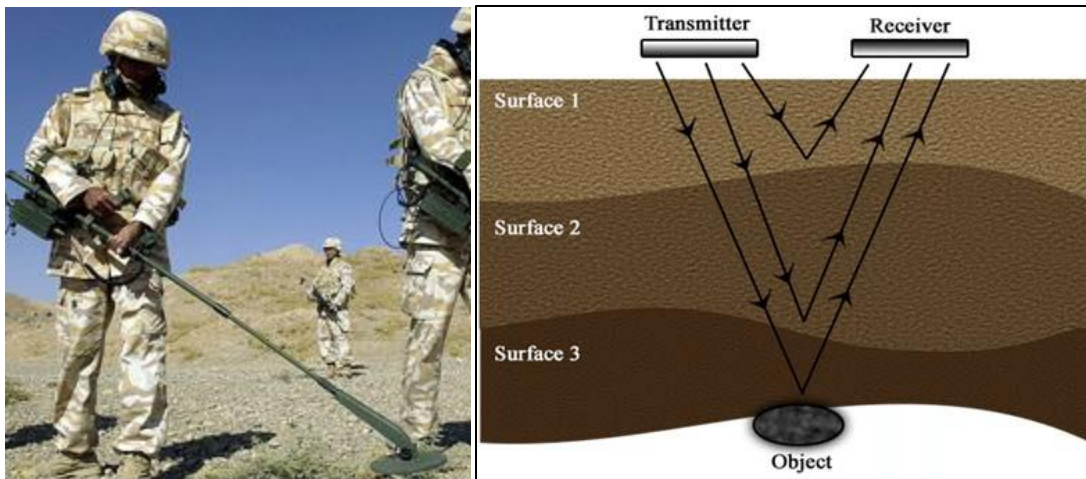
Figures 4 & 5: A Coalition Soldier looking for land mines in Iraq, principles behind GPR.

Ground Penetration based Radar

Legacy detectors above had difficulties in trying to detect trace amount of metals in mostly plastic polymer based land mines, this led to abandonment of employing specialized metal detectors for UXO demining operation. One of the newer techniques is GPR or Ground Penetrating Radar. GPR can detect buried clutter by sending a radio signal (10 Megahertz to 10 Gigahertz) into the soil and processing the return signals from reflected signal at any subsoil discontinuity with thresholds for phenomena such as soil-landmine surface boundary refraction, or soil-rock surface boundary refractions. This technique employs a transmitter/receiver antenna pair separated by a trivial physical distance for sending short radio pulses into the soil and recording any signals that return. These signals are then passed through a signal processing module to give a computerized pixel image determining shape and position of buried objects [18].

Infrared heat map based detection

In the Electromagnetic spectrum IR radiation lie in the region of 0.7 micrometer to 1 millimeter ranges. IR based techniques take advantage of anomalies or discontinuities in radiation possible due to many factors:

- Radiation reflected back by a buried underground object with some absorption in specific bands.
- Radiation absorbed by soil and vegetation around any buried object, most absorption will lie in the water bands.
- Radiation emitted by an active object or device, this is not the reflection of the transmitted signal.
- Background radiation from the sun, etc.

There are two modes of operation, an active transmission reception system and a passive reception within a specific range of wavelengths. An active system will have its own heat source and detects objects around it by processing the return signal and the discontinuities in it due to absorption or surface reflection. A passive method will detect radiations both emitted by a nearby object and from the background and visualize them. Thermal signal reception modules will take advantage of temperature differences in areas near any landmines as opposed to their surroundings. This is caused by many factors, the physical act of placing a mine will disturb the natural ground surface during the digging and filling, these disturbances will cause slight signal variations due to change in moisture levels around the mine vs natural vegetation around it, natural heat emission from an active mines, etc.

Acoustic/Seismic Resonance

A somewhat unique and unusual detection method based on mechanical properties of the mine surface as opposed to any electromagnetic behavior. The acoustic/seismic method comprises of detecting landmines by causing them to vibrate due to impact of the acoustic or seismic waves that are generated and received by No-contact (acoustic) and the Contact (seismic) transducers. A transmission module may be constructed using an acoustic loudspeaker, a reception module then senses the reflected signal and any presence of a signal above a threshold means a specific object such as a landmine may be present, this is because the amplitude of the reflected signal from a landmine will be far higher than a background signal as the transmission was made to get a forced resonance response from the land mine surface [19].
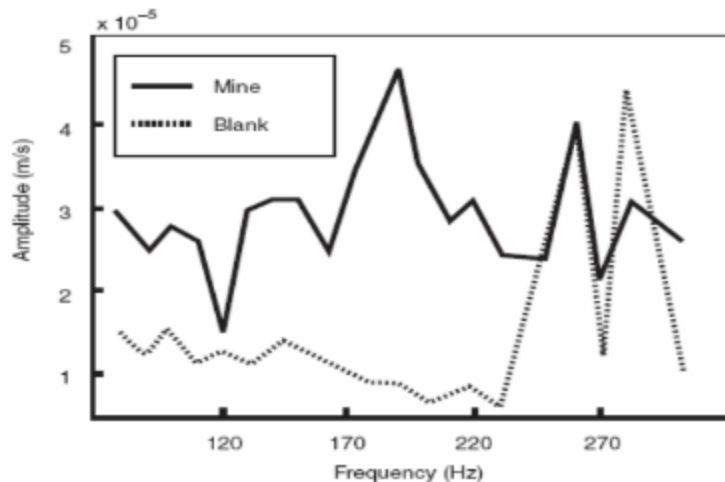
Figure 6: Amplitude of response vibration (reflected signal): blank (dotted) vs landmine (solid).

Nuclear Resonance Response (NQR)

This is another technique that takes advantage of resonance response. A radiofrequency signal can detect a specific chemical such as an explosive within a landmine. An emitter transmits a radiofrequency signal corresponding to the resonance frequency of an explosive compound. This will cause the chemical's nuclei to excite, emit a response and then return to their stable states. This response signal will induce a potential at the reception coil triggering an alarm due to an explosive being present [20].

Chemical Detection

As explosives are volatile by nature, trace amounts manage to escape through any holes and fissures as vapors. This technique detects presence of chemical vapors from an explosive compound. The technique has two approaches, a biological one such as employing use of a trained organism like as a dog to smell and detect explosives.

The other is a chemistry based mechanism for investigating low concentration vapors in air/soil samples collected in highly sensitive detection devices such as odor sensor, mass spectrometers, etc. The idea is that when the sample containing explosive is passes between the sensors, the chemical explosive contained will bind itself or react with a chemical present, this reaction of the present explosive might give off signals such as florescent light, a heat signal, change in mass of the solution, etc. thus confirming its presence.

Brute Force

Finally, there is always a hammer big enough to nail down the problem, in rare cases, if the terrain is suitable (such as a flat desert in Iraq), huge unmanned armored vehicles can be run over the field to trigger the mines. This technique is most preferred by armed forces during wartimes when time required to identify and isolate mines is simply unfeasible. It is the most expensive but least time consuming technique so far but leaves catastrophic scars on the environment,

10

leaving the mined areas destroyed. Furthermore, explosions may sink some mines deeper or damage them thus not triggering them, so there is no guarantee that the area is safe to inhabit later.

1.6   Related Work

This section aims to describe various projects that worked on landmine detection using multi-spectral IR signatures. Many of the works presented here were published in conferences, journals an articles and we have made sure to credit and reference them as clearly as possible. Many military researches have also been presented, this list is not exhaustive and some details or projects are missing both because of secrecy and lack of information.

Defense Research & Development Canada (DRDC)

This was one of the first "Mega" projects on landmine detection using images taken in Infra-red. This project was part of the R&D on unexploded ordinance identification in support of the Canadian Army 1978. The project studied target detection using IR optical and response images. Solutions developed in the project were applied to pre-processed datasets of multi-spectral images. An early milestone was a hierarchy based Computer Vision algorithm identifying sparsely distributed regions of bright pixels in a greyscale image [21]. Pre-processing steps were introduced to remove noise, overlaps in regions and several errors introduced by the imaging equipment. Un-interesting regions were discarded to compress the data. Suspect regions were divided into sub regions for homogeneity and feature extraction applied. A supervised classifier was applied to determine mine like objects and provide a probability of likelihood. The entire technique could be carried out in real-time if the mines were surface bound but not if they were buried. The initial goals were to develop a solution that can work in real-time and secondly to improve on the computer vision algorithms to get better processed data images.

Several Experiments with VNIR (visible & Near Infrared) cameras were performed and it was discovered that the spectral signatures of surface laid object are almost constant even under different lighting conditions and scales. From the research itself, in a more formal manner, a linear relation exists between incident lighting settings and mine signatures if the spectrum is confined to 500-680nm [22]. The research also concluded that Anti material mines were more observable and prominent than their Anti-personnel counterparts primarily because of their greater size and greater required burial depth [23]. The authors of [23] also measured that their probability to detect mines all over the dataset was between 0.33 - 1 and their False Alarm Rate or wrongly classified mines per meter square was between 0.1 - 0.52.

The next research focused on the effects of spatial parameters on the detection accuracy [24]. It was proven that as the size of the pixels approach the object itself, it becomes easier to

isolate/segment the object [25]. The research was performed using 2 sets of VNIR images, the first was taken in normal resolution at 300 meters, the other set was taken with high resolution at 6 meters. The normal resolution set had a FAR of 0.00034/meter squared. The higher resolution performed poorer at 0.0043/meter squared.

Another research [26] proposed a two mode architecture to detect surface mines with VNIR images, in the first mode, the system would learn and store the signature of target objects. In the second mode, the system would acquire target signatures and use comparison techniques between input pixels and stored references. Probabilities of match would then be displayed to the operator along with the image. This technique could be executed with 5-10 clock cycles of the input, where a cycle was defined within 15-30ms intervals. The process was also independently executed over every frame/chunk of the image so result were not affected by other frames.

The Author of [27] continued the previous research [26] aiming to modify the system to work with airborne reconnaissance systems in real-time. It first applied radiometric corrections over raw images and applied classifiers over the modified images. The concept of signature library was introduced and the results were displayed in real-time. The display illustrated results in selected bands. Detection accuracy was not the primary concern of this research. The goal was to test the viability of IR signature based detection in real-time from a flying aircraft. Due to the classified nature of the research no empirical data or indications were provided.

A research was also conducted to test the viability of using IR images in [28] Short Wavelengths (1000-2500nm) and [29] Long Wavelengths (7000nm). In the SWIR experiment, the detection accuracy increased as a wider band/spectrum was selected but the experiment failed to detect objects that were buried long ago/dated. LWIR experiment was performed over surface and buried mines in a variety of desert terrain conditions and performed better than broadband image systems in the category of buried mines [30].

The DRDC jointly conducted another project called Shield ARP to develop a real-time optical IR sensor technique for airborne explosive detection. The project combined SWIR and VNIR imagers to simultaneously capture data in both band. This gave improved ability to detect camouflage coatings on mine surface from the clutter. The project described the process and the results in an abstract manner but no details on the algorithms were provided [31].

Improved Landmine Detection Project

ILDP or Improved Landmine Detection Project aimed to combine various landmine detection algorithms to check if False Alarm Rate could be reduced. One of its key observations being that one technique alone would not be able to work flawlessly in all types of terrain and weather [32], furthermore able to detect different types of mines [33]. The project tested a remote operated vehicle with four different detector embedded into it.

- Electromagnetic Inducer
- Ground Penetrating Radar
- Infrared Imager
- Thermal Neuron/Bulk Activation Detector

This project aimed to detect Anti-Material mines rather than AP mines due to the size of the systems involved and low mobility. The technique was to work in the following algorithm:

1. Short Wave Infrared camera would detect a thermal difference between the mine and the surroundings.
2. Visible and Near Infrared Imager would also detect spectral signature differences of the disturbed soil and its surroundings.
3. Nuclear Imager would confirm or reject the IR images.

As the amount of images from four systems working simultaneously was very large, the authors decided to compress the data. Multichannel response images were converted to single channel greyscale images. The theoretical details and the results of this project were published in [34]. A key observation was that while in VNIR the signature differences were not large enough to distinguish, the reflectance responses were large enough to classify the objects.

Hyper Spectral Mine Detection

The Defense Advanced Research Project Agency or DARPA of the United States also conducted various projects under the HMD program, this like the DRDC is one of the "Mega" projects in this domain.

In [35] an experiment is conducted using Mid-Wave and Long-Wave Infrared bands. The project focuses mainly on soil disturbances and surface discontinuities due to mine burial. The primary reason of utilizing newer bands rather than VNIR or SWIR was the high false alarm rates introduced due to rocks and vegetative clutter.

The experiment was extended to detect buried explosives using contrasts in thermal responses in mines and rocks in the two selected bands [36]. The results showed that buried explosives came on the response images as bright noisy spots as the disturbed surroundings had a large surface temperature difference compared to undisturbed vegetation.

A sub project within the HMD called the HMD-P or HMD-phenomenology program was started to determine IR spectral characteristics that contribute the most to a successful landmine detection [37]. This resulting in collection of large amount of high quality spectral signatures of mines and clutter. The project performed several corrections over this data under varying controlled variables. The spectral signature analysis over this data is presented at [38]. Several observations were discussed, uncontrollable variables such as rain and wind were primary

contributors of varying results. Landmines affected by rain still however produced a signature that was largely different from the clutter around it. The recorded observations were as follows:

- A small shower will not affect the signatures.
- A shower of at least half inch rain is required to reduce the signatures in any meaningful way.
- A full inch of shower still does not eliminate the "distinctiveness" of the signatures.
- In low vegetative terrain, even several inches of rain will not eliminate the "distinctiveness" of the signatures.
- MWIR is the least performing band in IR responses.

Joint Multiple Spectrum Sensor Project

This project [39] aimed to test the different hyper spectral cameras to obtain information on best imaging systems to meet the conditions required for target detection. From a military point of view, it was necessary the cameras take images invariant to lighting conditions as the system could be employed both during daylight and nighttime. It also required the images to be taken across the Low and Medium wave Infrared channels because these bands have proven better observations considering background clutter signatures. The authors of this project proved that the best cameras should select small bands between 8 and 10 micrometers and use both LWIR and MWIR instead of just one band. The authors of this project also manufactured a camera SEBASS based on their findings.

Fusion Experiment

This experiment tested object detection based on simultaneous response collection in VNIR and SWIR wavelengths. The report concludes that fusion of just these two wavelengths has been just as effective in segmenting man-made objects from vegetative surroundings as simultaneous data collection in all spectral bands [40]. The results also showed that results were relatively accurate irrespective of lighting conditions.

Nightvision & Electronic Systems Directorate

NVESD of the United States conducted a series of experiments on aircraft mounted IR camera systems for landmine detection [41]. The systems were designed by University of Hawaii and took images in the LWIR band. NVESD also tested the compact airborne hyper spectral sensor or COMPASS which they designed themselves. The project tested two approaches towards classification. Signature based recognition or anomaly detection. Within the anomaly based

detection, they tried a local anomaly detection and global method. The authors employed use of a Stochastic Target Detector STD which outputs a detection stochastic map. This was then passed through a threshold to predict the classes. The entire project tried to detect landmines at sub pixel phase and relied greatly on the quality of the cameras.

NATO landmine project

This is one of the 3 "mega" projects, others being the DRDC and DARPA. The research was based in the Netherlands and objective being a UAV or drone mounted system that can detect landmines during an active conflict in near real time. The research is classified but a part was published at [42]. The research is very thorough and tested all technology available today such as Ground Penetrating Radars, Microwave cameras, LWIR, VNIR, MWIR, SWIR cameras, etc. The author of the published literature also gave some observations on their findings.

- Off the shelf medium resolution cameras are not suitable for detecting landmines in remote locations.
- VNIR cameras are small, low cost and relatively high performance, they can be used in real time conditions.
- MWIR and LWIR deliver rugged and acceptable results.
- Weather conditions can severely affect mine detections in MWIR and LWIR even if multiple bands are used.

Other Major Landmine Projects

The Humanitarian Demining or HUDEM is a demining research project based on multispectral and multichannel data relying on sensor fusion (GPR and IR). One related paper published on this project [43] discussed the potential of this approach. The project takes a probability and prediction of class model with an analysis of the data from the primary sensor in the first phase, in the second phase the data from the other sensor is then fused. Finally the decision about the classification of the object is left to a human observer, the project only provides a probability. One observation is that this fusion provides a better performance than relying on one sensor alone.

The Swedish Army, following its policy of self-reliance started a project of its own termed MOMs or Multi Optical Mine Detection System. This project was partly influenced by the HUDEM approach and followed a similar algorithm of rapid detection of surface bound objects using multiple sensor fusion [45]. The published results conclude that the performance is unsatisfactory for painted and camouflaged objects under cover of nearby vegetation/terrain, similarly no approach works under all terrain conditions and results vary widely [43].

A landmine detection project was also started by the DSTL in the United Kingdom similar to DRDC & DARPA, the other two "mega" projects. Unfortunately due to lower budget funding and a parallel NATO funded project, this was cut short. The authors published their findings at [44]. The project employed use of an off the shelf SOC-700 mounted camera for taking high quality landmine images. This data was then processed to try different image processing techniques. This project had no interest in the accuracy or the false alarm rates. The authors suggested the use of Principle Component Analysis to reduce the dimensionality. The authors also concluded that comparisons of target and pixels of the images would be a time and resource consuming method and hence better avoided.

The Indian Army funded several projects to detect landmines using Infrared images. One such project was conducted and published at [46]. This included several pre-processing steps such as smoothing, filtering, contrast stretching. The project was deployed on two types of soils, harsh sand and black cotton clay. The image was converted to greyscale and its contrast stretched. The authors then segmented the images based on regions of interest (ROI). Finally they applied a Neural Network for classification with 4 neurons and 1 hidden layer. The project is very simple and only in its preliminary phase.

Chapter 2

2.1   Infrared Signature based Detection

Rapid development in optical imaging electronics mean that contemporary imaging systems can acquire a scene simultaneously across thousands of wavelengths also known as broadband imaging. A modern off the shelf camera today can slice an image into bands so narrow that they qualify as a continuous spectral image rather than a discrete set of spectral images clustered together, much like an RGB image compiled together from three discrete "channels" or images, but on a much broader scale. Before we continue, it is important to understand the operating principles behind Infrared Object Discrimination and how a detection technique can be based on these thermophysical phenomena.

We begin with a clear observation that landmines and the soil that surround it have different thermal and physical properties and will reflect, retain and emit heat differently based on the composing elements, in short the rate of change of heat for a landmine will be different in regards to its surroundings and we will employ use of a sensitive camera that can record temperatures of these objects in short intervals to give us a spectrum of its thermal behavior. The primary reason behind the difference in rate of change of heat in the landmine in contrast to soil is its unique thermal capacitance, one of the quantities comprising an IR signature. Two objects with

similar thermal capacitances will have IR emissions so similar that it will be extremely difficult to distinguish between them based on thermal signatures alone.

Other primary factors also come into play such as the size of the landmine we target and the depth at which it is buried. The terrain and geography also come into play as does the time of the day the experiment was conducted, there will be a lot of thermal noise in an experiment conducted for example during midday of July. One primary observation forms the basis of IR based detection, surface temperature changes directly proportional to change in radiation [47]. This can be explained in the following way, as the sun goes down, the surface temperature will change proportionally to the incident IR radiation received from sunlight, or if we change our device configuration on the IR camera, surface temperatures of the objects in the image will change and more importantly, surface temperatures of mines will have no difference in regards to depth over small distances, a mine buried a few cms from the soil has the same surface temperature in the image as one buried 2-3 feet underground.
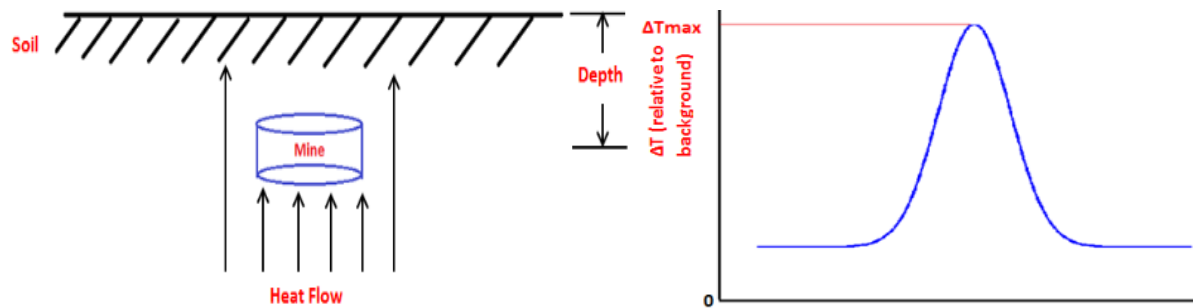

Figure 7: Thermo physical capacitance leads to Infrared Signatures

On closer inspection, the laws of thermodynamics state that any thermodynamic system aims to achieve equilibrium as observed that any noise due to solar heating will overtime cool down during the nighttime. Consequently as the depth increases, temperature increases, thus the theoretical maximum depth flooring will not depend on the most expensive IR sensors, a camera with just enough spatial resolution to cater to the operating depths of the landmines will be enough.

A spectral signature is a specific reflecting/absorbing behavior a material/object shows with respect to EM radiation. It records the changes in the reflectance as wavelength is altered. In more formal terms the spectral signature of a material in question is a function of 2 variables, the incident EM radiation (wavelength) and the reflectance/emittance ratio exhibited by the material as a response to the incident radiation. These measurements can be made with a very vast variety of instruments the discussion of which is beyond the scope of this section. As behaviors change in different ranges of the EM spectrum, it is often best to isolate the behavior at the region of interest. The signatures also need calibration i.e. application of various correction techniques, the first one to be is usually illumination, which can only be avoided if the signatures were recorded under a specific illumination in a lab. Finally, depending on pixel resolution, it is

often better that a pixel represent many spectral signatures banded together/average of the behavior across several experiments to minimize recording of noise.
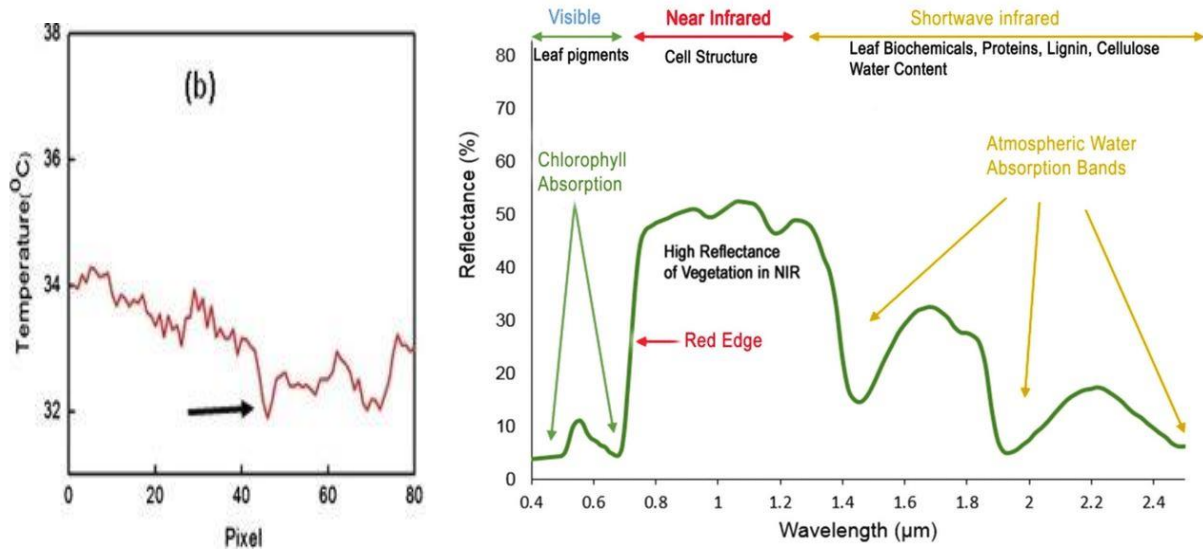
Difference between a heat map curve (left) vs a spectral signature curve (right).

A generalized IR signature based detection approach is presented here, this is not specific to Landmine detection in itself but several steps will need to be added to cater for domain specific problems as we will see in the coming sections. In our case our first step is to collect a broadband image to serve as the data, a typical off the shelf camera available easily on the market is assumed here. Such a camera according to general specifications [48] will take an image at a resolution of 256 by 256 for a 1.16m square target, which calculates to 4.5mm pixels. This is followed by a resampling by using a 25mm square filter kernel, kernel averages are assigned to the grid cells resembling an image convolution operation.

The second operation is the "proposal region search" where high contrast regions are selected as potential regions containing features we desire. A third operation will require any contrast stretching technique of our choice to be applied locally and cell values/intensities presented after the CE technique removes background noises and enhances cell values within the proposal regions. Finally and optionally a bounding box can be drawn around the objects by utilizing both the proposed regions and cell values/intensities obtained at those regions from step 3 as part of the output through a segmentation technique of our choice and applying thresholds over feature vectors, etc. Finally there is a probability based classification over the results to decide if an object of interest is present. Note how much quality improves during the image enhancement steps.

Figure 8: An off the shelf IR camera with PCI Board, A typical image after resampling and final output.

This technique can be used at various scales, a small camera connected to a PCI board with a storage device or a lightweight laptop can be put in a bag and hanged to a flying drone to locate and detect anti-personnel landmines in real-time with the above mentioned technique as these have relatively small operating ranges and thus buried very close to the surface as opposed to the larger AT mines with more operating range. Indeed we point out to such an experiment carried out as field experiment in Northeast Bosnia after the Serbian wars at a suspected minefield [48].

This field was a small farm that was already demined and used for training purposes. It was divided into 5 lanes of 50 meters each with increasing difficulties as several inert landmines inserted at increasing depths from 1 to 20cm. The experiment referred here was successful, 100% for lanes 1-3, 93% for lane 4 and 69% for lane 5. For a large scale experiment, far more processing time will be required along with several layers of image enhancement techniques although the structure of the technique will remain largely the same.

There are several outlets to obtain practical live acquired spectral field images from open source image libraries, many of them funded by various governments across the globe. We mention a prestigious such collection, AVIRIS or "Airborne Infrared Imaging Spectrometer" operated by NASA's Jet Propulsion Lab (JPL), it comprises of a specialized high altitude aircraft (such as U2/ER-2 and WB-57) with fitted onboard sensors and Imaging equipment acquiring imaging data across 224 continuous channels between 400 and 2500 nano-meter ranges, with spectral resolution as precise as 10 nanometers. It has a row of simultaneous cameras and acquire images perpendicular to the aircrafts fly path. Images are collected in batches or rows. AVIRIS's camera suite has an Operating view of 30 degrees mapped to 614 pixel image. Data collected during flights are openly available at [49]. We do mention though that the images only cover the terrain and any minefields will need to be "simulated" and thus are of limited utility in our case.

It is most convenient to choose a live acquired image set with real landmine signature responses in contrast to a "simulated minefield". " Here we also see an advantage of using IR response images, modern land mines are made of plastic and often are painted to camouflage them to their surroundings and consequently not detectable using Visible Light images, especially if the

landmines are buried deeper than a few cms. As we will see in the next sections, a landmine's signature may camouflage or appear close/indistinguishable to that of its surroundings in many bands of the spectral image set, signature contrast will however be visible across other bands and a mine can easily be distinguished across a large and finely prepared dataset.

Before we can move further about landmine spectral signatures and their properties to build our approach, it is important to understand about IR electromagnetic responses and the theory of such datasets acquired from several sources.

2.2   Dataset Preparation

The scope of the practical implementation of the project is limited to small AP plastic mines with the following assumptions:

- Composite AP mines are small targets and consequently most challenging to detect.
- AT mines are larger, easier to spot and difficult to trigger and not as dangerous to civilians as AP mines.
- AP mines were massively deployed in recent conflicts (Soviet Afghan war, War on Terror, etc.) and are still a major challenge to the Afghanistan-Pakistan region within the scope of the thesis.

Our primary focus for the thesis is the US Army standard BLU-43 AP mine and the Soviet reverse engineered copy PFM-1 Butterfly. It has a polyethylene plastic manufactured casing and weighs 75g. It is extremely lightweight and can be scattered or aerially deployed [50]. It has notoriously difficult and expensive manual clearing techniques due to its unique design as we will see further.
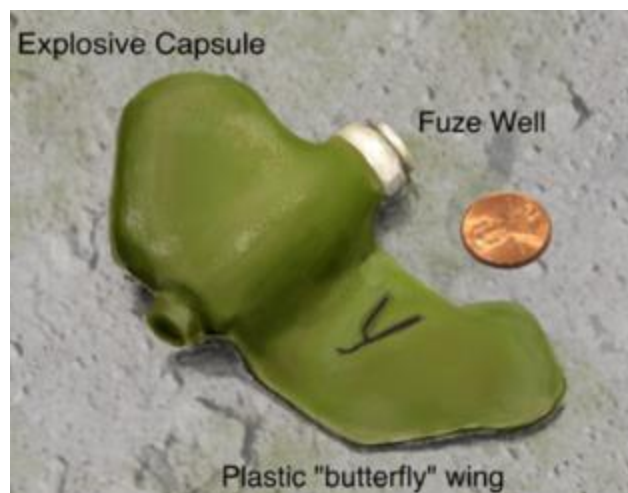

Figure 9: Inert American BLU-43 shown to scale, instantly recognizable and appears as a toy to children.

The butterfly was a primary engagement weapon during the cold war and was deployed in the millions during the Soviet Invasion of Afghanistan during 1979. Even presently they remain relevant as the Russian Armed Force inducted a modernized variant of the PFM-1 into service, there are several Russian minelayers and heavy equipment specifically tailored to be used with PFM-1. A UMZ-G (multipurpose tracked minelayer based on T-72 or T-90 chassis) can deploy more than 15 thousand butterflies in less than 1 hour [51]. While the PFM-1M (modernized variant) is supposed to self-destruct upon expiration time, older PFM-1s had cheap, low quality fuses and open did not self-detonate upon the expiration of expected deployment duration, Recent studies[52] show that less than 48% PFM-1s self-detonated upon reaching their expiration period.

The design and the manufacturing of PFM-1, as well as their deployment violates the protocol II of UN CCW (Convention of Prohibition of Certain Conventional Weapons) and their massive deployment during the cold war and continued usage within the Russian Army constitutes a major humanitarian concern [53].

Faithful to their design (camouflaged area denial weapons with long shelf life), there remains a lack of time/cost effective standard tactic to safely identify deployed PFM-1s. Recent induction of cheap flying drones that can be equipped with Thermal Cameras are a breakthrough in an otherwise stalemate. IR signatures obtained from high resolution Thermal cameras can allow high accuracy analysis of the texture and finish of the PFM-1s poly ethylene plastic case, differential averaging of IR signatures can help determine a TI (Thermal Inertial) or thermal signature. Other parts of the mine such as the KSF-1 (case-rail) and the blasting caps can help calculate a more accurate signature.

A faithfully compiled, real imaging dataset such as the MPG or the Milbrooks possesses the following properties to make it an ideal tool towards training a solution on it:

- Dynamic imaging that can be used in a variety of terrains and scenarios.
- High accuracy data yielding large temperature differences between similar elements of the environment (rocks and soil).
- Several variables can be evaluated over a well-tempered dataset. These may include time of the day, humidity, geology, season, etc.

From a thorough study of a small AP landmine's signature [54], it is concluded that ideal thermal conditions for detection of any small AP landmine such as the PFM-1 mine occur:

- 2 hrs after dawn or at high noon or around midday
- After a rain spell due to increased moisture retained by the environment around the landmine, leading to an increased temperature difference between a plastic cased landmine and wet foliage, It is calculated[55] that water's heat capacity is 4.186 joules per gram Celsius J/gC and is absorbed by the soil but not the plastic casing.

- In desert areas as the finely grained sand decreases the probability of a false alarm against even a lightly vegetated grassland as any foliage is potential cover to the landmine.

It can be said that an ideal cost and time effective solution to detect scattered pockets of deployed PFM-1s in a potential minefield would be a UAV mounted Thermal imaging set coupled with a well-trained automated object detection module such as a NN architecture (neural network) as the majority of work, image surveying and segmentation and classification of an object in an image by a manual operator would be a huge time and resource bottleneck and thus an operator should only need to pre-process the images acquired by the UAV set and ready it for interpretation by the NN module.

Recently, Modern GPR suites have updated sensors and the imaging systems has far more complex. The file sizes are considerably larger due to huge number of added bands. The dataset's headers have a list of number of bands or lemdas. There is a tabulated dictionary for the bands per region for further use. The GPRs need to be calibrated based on the EM region/band they will operate in and decide the characteristic wavelet (signal sent into the ground). Before the dataset can be acquired the GPRs also need to perform time calibration (for taking images in regular intervals) and frequency filtering which would reduce band noise at the corner frequencies. Band dictionaries will also be useful because the characteristic wavelet must have adequate penetration ability w.r.t the operating depth at which we expect our targets to be buried. The operating bandwidth must also be wide enough w.r.t our expected image resolution e.g. a small bandwidth will not have sufficient scattered response signal from the target object to form an image. There remains a trade-off between the signal strength, operating depth and image resolution, the GPR can lower the operating frequency to archieve higher penetrations or lower signal loss but this then reduces operating bandwidth which will result in lower resolution and decreases discrimination increasing false alarm rates. Changing terrains will also change signal absorption. Thus careful study of experimental parameters and system characteristics is required.

Out[4]:

	Band number	Band center (nm)	EM region
1	1	376.86	visible-violet
2	2	381.87	visible-violet
3	3	386.88	visible-violet
4	4	391.89	visible-violet
5	5	396.89	visible-violet
6	6	401.90	visible-violet
7	7	406.91	visible-violet
8	8	411.92	visible-violet
9	9	416.93	visible-violet
10	10	421.94	visible-violet

Figure 10: Tabulated bands along with their centers and Spectral locations

As see above there are a lot of regions, most of which beyond the scope of the requirement that is Near IR region.

Now we need to select the band/region of the spectrum in which we will operate. We will also need to compute our signal bandwidth based on the band center as discussed previously. GPRs offer a wide selection of settings and each scenario is best suited to one set of system parameters.

Firstly we need to convert the co-ordinate syntax into plottable image data (pixel locations and line data) from the UTM data. We need to export the image set object/shape file as a json string and then check the Meta data of the output function to make sure that their co-ordinate geometric projections are the same. For example the UTM coordinates are given as a [x y z] vector. If our object is converted successfully, their projections will match and we can use the following inverse transform to calculate our image pixel projections from the UTM format.

```
Xgeo = GT(0) + Xpixel*GT(1) + Yline*GT(2)
Ygeo = GT(3) + Xpixel*GT(4) + Yline*GT(5)
```

- where *GT* is the geotransform acquired with `img.GetGeoTransform()`

```
Site 1 UTM coordinates (x,y):           (454813.1341233433, 7179015.677325998)
 are equal to geographic coordinates (lng,lat):   (-165.94878999999995, 64.73281000000001)
 and fall within image coordinates (pixel,line):  (355, 1898)
```

As we calculate an inverse transformation function for a dataset, we can use a loop to convert any site as required. Now we can plot a response curve for a geographic site in the dataset for band N using image coordinates calculated above and converting them to integers.
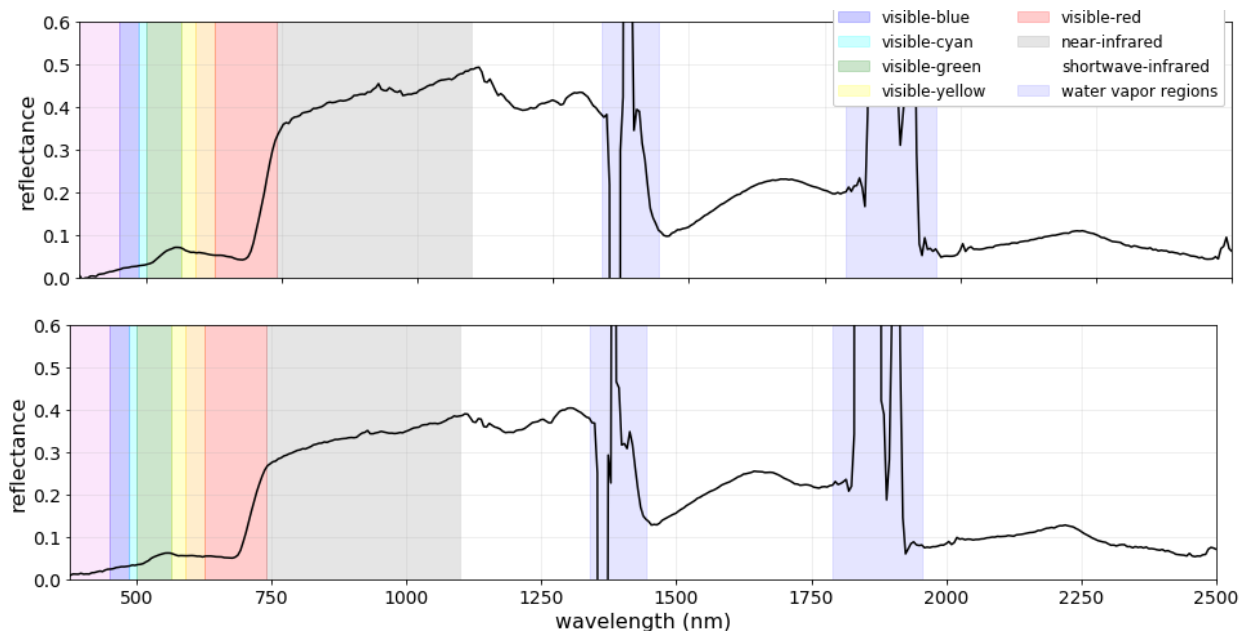

Figure 11: The color coded electromagnetic spectrum clusters and the IR region (Grey: 720-1100).

Note that shaded regions corresponding to their dictionary bands in EM spectrum have been superimposed corresponding to their regions in the curve. Thus for example we are only interested in the gray Near IR region of the curve. To utilize the IR Region specifically, we need to determine and isolate the bands that lie within the grey region and then stack them together.

Although landmines have been extensively employed all across the world in countless wars, to this day no region has suffered from landmines as much as Pak-Afghan corridor following the cessation of the Soviet Invasion of Afghanistan. During the invasion (Dec 1979 - Feb 1989) more than 15 million AP mines were scattered or buried across Afghanistan [56]. These mines are mostly still in their deployed areas primarily because of being too remote for demining. As time passes, these mines have deteriorated over time and how present an increased threat to local communities with little options of defusing them [57]. While there are no official figures to the victims of the landmine crisis, several experts suggest that the causalities are in at least several thousands of deaths and injuries since 1989 [58]. In the scope of the thesis, we have taken care to select datasets which were acquired over multiple varieties of terrain similar to the Western frontier areas of Pakistan and Afghanistan, locally known as the Pak-Afghan corridor. The reason being not only geographic relevance but also that some of the most extensively mined regions in Afghanistan are those that bordered Pakistan and Iran. This is almost exclusively also the case in Pakistani tribal regions that lie in the East [59].
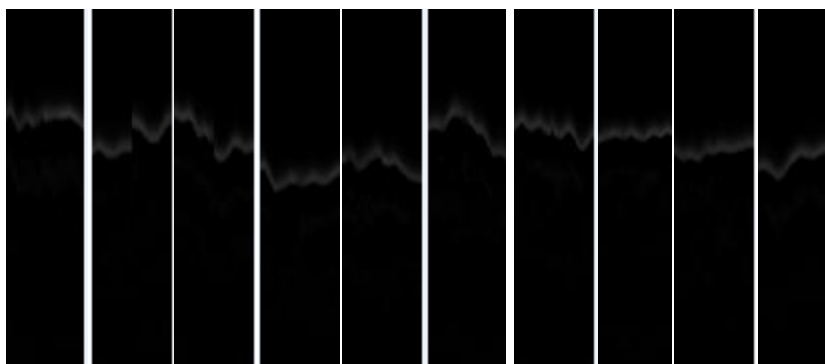

Figure 12: IR Spectral Responses for 10 objects, raw and unprocessed.

For this Project, we employed three operational datasets belonging to the Biometrics and Machine Learning Lab at the University of Florida. These are:

1. MPGSep2005
2. Small Millbrook
3. Tiny Millbrook

The first dataset comprises of 1791 images of while 496 are real landmine signatures. The Millbrook Datasets are compact datasets with 540 & 43 images. The datasets comprise of IR spectral signature responses from a GPR (ground penetrating radar) attached to a moving vehicle sending signals into the ground and receiving the responses if they hit a buried object. The datasets have been collected over several real landmine fields (real but defused landmines) with many types of buried targets over several terrains. We also received truth values about every image in the datasets, whether the spectral response contained in an image is that of a landmine or a clutter object (Non landmine).

All images have the dimension of a width of 40 pixels and a height of 415 pixels i.e. 40x415. This is because all 3 datasets were compiled by the same source using the same equipment, taking images at the same regular time intervals. We see below an Aladdin GPR with a bandwidth of 2 GHz and 2 bow-tie antennas 6 cms from each other. The signal speed is 14 cms / nano-second. The sensor module has dimensions of 12 x 12 cms and weigh 2 kilograms.

Parameter	Value
Inline sampling	0.4 cm
Crossline sampling	0.8 cm
Time sampling	0.0522 ns
Time window	20 ns
Antenna separation	6 cm
Antenna height	<1 cm
Antenna frequency	2 GHz
System bandwidth	2 GHz

Chapter 3

3.1   Multispectral Computer Vision Techniques

In this part, we will be acquainting the readers with the image processing algorithms implemented in various parts of the project. We will also acquaint the user with various pre-processing stages such as error reduction, noise removal and so on which are preliminary towards the final identification and classification stages. Many of these algorithms are not specific to landmine identification but were ultimately selected because they worked best, use of other approaches is debatable and relevant to the MS track chosen by the author.

Once the data is acquired, it needs to be passed through several preliminary stages. We need to remove noises and other errors or mistakes in the images such as blurriness, too sharp, contrast, etc. We also need to compress the images as much as possible to cut back on processing time later on. We need to smooth them, make several correction to errors introduced in various ways

such as background radiation. We also need to segment useful features from background clutter. We can think of the processes as having various phases with several steps in every phase.
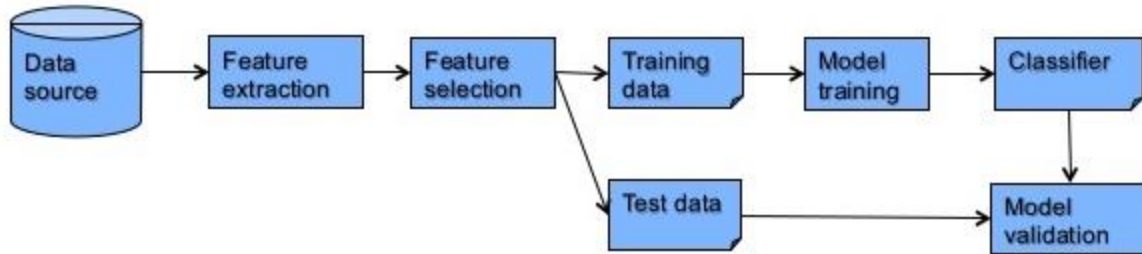

Figure 13: Pre-processing and Detection Process Flow

The pre-processing primarily focuses on three important tasks: contrast stretching, filters and smoothing/averaging. Our goal here is to remove as many impurities and noise from our data as we can while reducing the size and dimensionality of the data we will be working with without losing any context. Finally we segment useful information from the background clutter which can then be classified using common features. The next stages will be feature extraction to help classify isolated regions of interest and clustering techniques to help "tighten" the bounding box around it. We will review important concepts and techniques as well as the working principles that we implemented in the project.

Utilizing IR signatures exploit the property of the object's thermal contrast in respect to the background. All objects with surface temperatures exceeding that of absolute zero emit some IR radiation with lambda between 3 to 100 micrometers. The magnitude of this radiation depend on the temperature of its surface. Thus a landmine can be considered a thermal anomaly in the natural heat flow of the soil around it. Thus it will disturb the normal thermal pattern of the location it is placed. It is the presence of these anomalies that is used as an evidence of the presence of a landmine in the location [60].

A good IR sensor can detect a heat difference as small as 15mK (milli Kelvin) and give the difference as an electronic signal that can form a thermal image on which to perform pixel calculations. The role of the sensor thus being a detector possessing a transducer that converts the IR radiation of the landmine into an electronic signal. This detection is usually based on the rate of energy absorbed [61].

IR images can be processed in two ways. We can process a series of continuous images in a batch operation or we can perform static calculations on an individual image itself. A batch wise image sequence of a scene will have a temperature difference curve against time allowing observation of specific phenomena such as shape and volume, apparent surface temperatures at time T. The image taken itself can be taken with active or passive sensing. Where an active sensor has its own heat source and only evaluates absorption response for any objects around. A passive sensor will

26

sense only the IR radiation objects around it are emitting. Thus once the polarimetric IR images are taken, the processing and detection process will follow a sequence of steps from pre-processing to contrast enhancement to correction process to finally classification and identification.

In our case, the IR sensor was embedded on a GPR based multi sensor suite that while attached on a moving vehicle took images at constant intervals while maintaining specific angles over the target area. This filming was running continuously acquiring image sequences. Some detail is described to give the reader an appreciation of the process. Every finite distance interval travelled gives a pulse. Every pulse records a multispectral image against it. Thus the interpolation of distance pulses will decide the exact position of an image in a continuous sequence.

The suite enhances the detection by employing a polarization filter. It enhances the differences in thermal properties in the region and provides extra information about the objects (vegetation index, surface temperatures, etc.). Thus prediction of a thermal signature requires gathering key knowledge about several important phenomenon [62]:

- Heat Flux into the soil
- Thermal properties of target landmine
- Thermal properties of terrain and vegetation above and around the landmine.
- Cyclic noise of solar radiation
- Thermal signatures of any buried anomalies that may factor a peak.

3.2   Pre-processing and Image Corrections

There are several corrections an imaging system employs to improve contrast in a high clutter scene, however If the contrast of an object and the background is not acceptable, more processing is required because direct segmentation on a GPR signature image against a small object barely registering as a few pixel blob is not possible. We go through some of these correction steps.

Image Calibration and Correction: It is important to realize that the captured image will have noise added to it due to vibration of the camera. A simple solution is camera calibration. In every orientation of the angle, a hot and cold calibration is applied and the 2 calibrations provide us an offset and gain for each pixel. A convolution operation or offset correction then removes said noise from the image.

Radiometric Correction: As we know the image grey values are provided using the physical units such as (watt per square meter per steradian). The correction procedure will require using two

black bodies, one at room temperature and the other one heated. Now assuming that both bodies have uniform temperatures over their entire surface with emission coefficient as 1 are placed around the camera. The acquired image sequence will be corrected using equation 1 after the full sequence has been acquired.

Where bb1(x,y) and bb2(x,y) are the averages of black bodies 1 and 2 and r2 and r1 are the black body radiances given by Planck equation. Where lambda 1 and lambda 2 are lower and upper bound of camera's wavelength. The resulting image radiance is now directly related to the scene and corrections can be performed [63].

Figure 14: Equations 1 and 2

$$I_c(x,y) = I_{r1} + \frac{I(x, y) - I_{bb1}(x, y)}{I_{bb2}(x, y) - I_{bb1}(x, y)}(I_{r2} - I_{r1})$$

$$I_{ri} = \int_{\lambda_1}^{\lambda_2} \frac{2hc^2}{\lambda^5} \frac{1}{e^{\frac{hc}{\lambda k T_i}} - 1} d\lambda$$

Gaussian Filtering also called smoothing is a 2 dimensional convolution using a Gaussian filter kernel that blurs or smooths images. It is a necessary step to correct pre-processed image datasets with Gaussian filters as part of noise removal operations [64]. Furthermore multiple morphological operations can be combined to remove further noise and provide important processing such as contrast stretching, an example would be histogram equalization [65].

Pixel Fusion Techniques (PFT): Multiple images for the same scenery taken with different positions and angles of polarization filters will be combined with PFT to gather polarization data for enhancement processes.

3.3   Feature Extraction Techniques

Isolating shapes that resemble mines or other target objects is the first crucial step in the detection technique once the pre-processing corrections are completed. It is possible to detect and classify based on disturbances in the soil's thermal pattern caused by a buried object being present. This presence is unexpected and alters the pattern that was expected from that area based on signature averages of neighboring pixels. Based on our assumptions that signatures of landmines will be based on thermal reflectance/absorption properties of the casing they possess [66].

Contrast Stretching

An enhancement technique that tries to improve or better an image visually through a collection of methods trying to convert it into a form more suitable for analysis by a computer [67]. The methods can be classified into 2 main domains Frequency domain and Spatial Domain. Spatial Domain techniques directly manipulate and change an image's pixel values. Frequency Domain techniques first convert the original image into frequency domain with the Fourier transformation, edits it and then converts it back to its original (spatial) domain at the end. Contrast stretching is one of the most common enhancement method and is pretty much mandatory for machine learning based solutions. In our case, the role of this step would be to enhance the differences between the thermal signatures of landmines and surrounding terrain, as its name implies to "stretch" or increase the contrast of the images [68].

Histogram Equalization

HE is one of the easiest techniques to archive contrast stretching because of its simplicity. The goal here is making the probability distribution of the image grey levels roughly uniform. It operates globally on the input image and flattens and uniforms the grey level distribution using a cumulative probability density function [68]. As stated above the goal is to obtain an output image with a uniform grey level distribution histogram which we can archive through use of the following function with its two working properties:

$$g_k = T(f_k) = \sum_{j=0}^{k} \frac{n_j}{n} = \sum_{j=0}^{k} p_f\left(f_j\right)$$

(a) $T(f_k)$ is single valued and monotonically increasing in the range $k \in [0, L\text{-}1]$.
(b) $T(f_k)$ should be $T(f_k) \in [0,L\text{-}1]$ for $k \in [0,L\text{-}1]$.

Figure 15: Histogram equalization function with its two conditions.

There is one catch so to speak with HE being that this technique changes the brightness of the image, to battle this several SOTA variants of HE are recently introduced such as Dualistic sub-image Histogram Equalization(DSIHE) [69]. The following figure shows histogram equalization in action notice the uniform distribution function in the second image. An 8 bit flag for grey levels indicates 255 possible grey levels or "colors" as seen in the x axis.
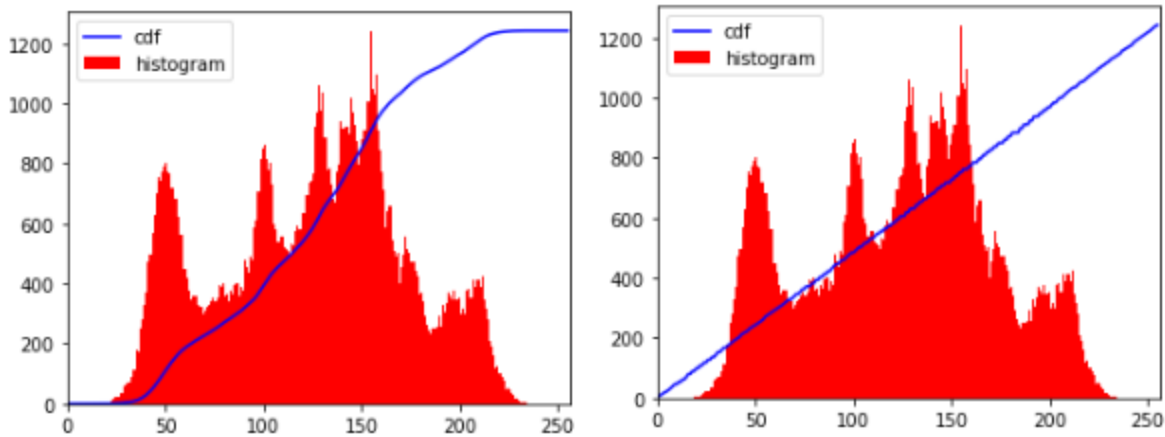
Figure 16: Grey level distribution histograms before and after histogram equalization over the image.

Filters

Filtering is a process where the image is convolved with different filter kernels or "filters" to archive some specific effect on the image. Many filters allow noise reduction and sharpening blurred areas of the images, etc. Making our images clearer and tailoring them for better results. In our case however, filtering hyper spectral IR images will require multiple channels to be filtered simultaneously. We have two types of filters available, the first type of filters work on the condition that channel specific data is separable from cross channel information or in technical words: spatial and spectral data is separable. We call these "hybrid" filters. We use these filters in a two-step process. First we decouple the different channels using principle component analysis and then use classic convolution operation over individual channels, finally recoupling them using their component weights. The second type of filters do now rely on the assumption of separable spatial and spectral data as they rely on both simultaneously [70].

Segmentation

In a more formal manner, this is a process that searches for homogenous regions within a given image [71]. More casually, we are looking for "interesting" regions within our image that we can later classify. There are many image segmentation techniques available but few of them are applicable for hyper spectral data. There do exist methods like the watershed segmentation that have variants that can work with segmenting hyper spectral images. In a more rigid context, we can divide all segmentation techniques based on their working principles as boundary based segmentation or region based segmentation. The Boundary based segmentation detect boundaries in an image taking note of pixel patterns and finding discontinuities. The region based segmentation clusters pixel based on "similarities". We will go through some of the best candidate techniques for our case.

Watershed Segmentation

This is a powerful morphology segmentation algorithm. The authors [72] provide the explanation of the variables used for segmentation namely spectral markers and spatial gradients. The approach is summarized below.

- Use of gradient function when flooding to avoid getting a lot of minima.
- Determine markers to each region using Clara Clustering Technique [73].
- Utilize FCA (Factor Correspondence Analysis) to remove redundant channels [74].
- Filter the image using FCA.
- Compute Chi-Squared gradient over the filtered image.
- Finally compute the watershed based segmentation.

As introduced in previous sections, this is a topography based region growth technique. The landmines are taken as anomalies in vegetation or terrain textures. The approach can be summarized as isolation based on parameters of patches of textures and clustering of those patches.

Feature Extraction

This process aims to reduce the dimensionality or dimensional space of data while trying to conserve as much info and context as possible. In our case, it would try to help with the problem of having a small number of training images compared to their high resolution, effectively cutting back on computing time. Feature extracting algorithms may or may not be linear and unfortunately for us, not all of them are even useful to begin with.

Feature Extracting Techniques isolate useful data from the input sets. In many cases, only removing redundant values alone reduce the dimensions of data by a significant factor. Some techniques focus on the surface and texture of the objects while most of them rely on the shape and orientation. In our case, the Local Binary Pattern (LBP) and Generalized Region Assigned to Binary (GRAB) will deal with object's textural data while the rest of the extractors will deal with spatial orientation and shape.

Principle Component Analysis

PCA also known as the Hotelling or KL (karhunen Loeve) transform is a popular dimensionality reduction technique working on the concept on representation error minimization. Our goal is to identify principle components or most contributing regions in an image using eigenvalue decomposition from computing the covariance matrice form the image [75]. These principle components can be thought of as linear combinations of the original variables and most of the

information in the image is thought to be squeezed into the first k components computed. Imagine a 5 dimensional data giving us 5 PCs (principle component), the PCA will be trying to squeeze maximum info possible into the first component followed by squeezing as much of the remaining into the next (2nd) and continuing as illustrated by the figure below.
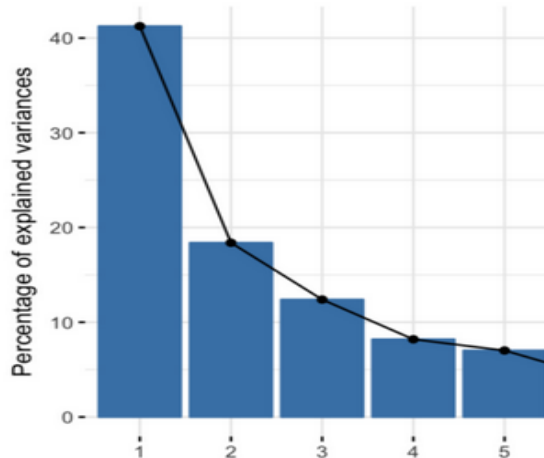
As seen above we have the number of components in the axis against their "weights" or contributions in the y-axis, we can see that much of the image's context is contained within the first 5 principle components evaluated.

We will try to summarize the working concepts. Firstly PCs always equal the number of variables in the data/equation. PCs are always computed in a way that the 1st PC represents the largest possible variance in the set. We continue the same way adding once condition that the 2nd PC is perpendicular and thus non-correlated to the 1st PC. We stop when we have k PCs equaling the initial number of variables. As we know eigenvectors and eigenvalues come in pairs i.e. for every Eigen-vector we have its corresponding Eigen-value and their numbers coincide with the number of dimensions or dimensionality of the data. As the eigenvectors of the co-variance matrix computed on the data give us the direction of the axes with most variance (most info) which we call PCs. We can say that eigenvalues are then coefficients of the eigenvectors that tell us the amount of variance represented by each PC. If we arrange the eigenvectors in mathematical order of their eigenvalues, we get the PCs in their representative order of significance.

$$v1 = \begin{bmatrix} 0.6778736 \\ 0.7351785 \end{bmatrix} \qquad \lambda_1 = 1.284028$$

$$v2 = \begin{bmatrix} -0.7351785 \\ 0.6778736 \end{bmatrix} \qquad \lambda_2 = 0.04908323$$

Imagine a 2 dimensional data with the eigenvector-value pairs of the covariance matrix as above. We see that lambda 1 > lambda 2. We know now that vector v1 corresponds to PC1 and v2 to

PC2. It is an established concept the total variance in data always equals the sum of eigenvalues. We can now get the representative percentages of the PCs by dividing their corresponding eigenvalues divided by the sum of the eigenvalues giving us 96% and 4% for PC1 and PC2 respectively. In theory, we will with each PC be getting a classification pattern against which to classify objects of interest.

From our implementation view, the PCA (Principle Component Analysis) was used mainly to reduce a lot of different sources of noise mainly AWGN or Additive White Gaussian Noise, improving accuracy gains, it also simplified/damped the signature responses especially the regions with high amplification, before they were analyzed. Other sources of inaccuracies included:

- Soil Clutter
- Air-Terrain bounce
- False targets
- Signature Reflection.

PCA is an important part of pre-processing precisely because several minute anomalies and error sources contribute as false targets, increasing the FAR or false alarm rate.

Moving on, passing an interpolation technique over a chunk/cluster of signatures followed by PCA will result in a far smoother contour map being drawn, one example is illustrated below. The left diagram illustrates raw chunk of signatures, the right diagram illustrates the same chunk after PCA has applied damping and removing various sources of noise described above, mainly AWGN.
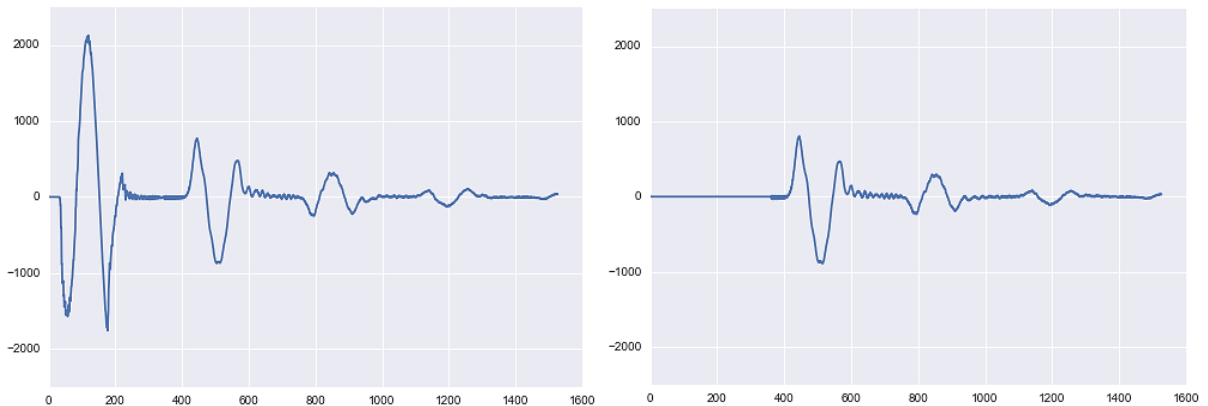
From here, it will be trivial to compute the Eigen variances/ Eigen data for the smoothed signatures. This will also help better compute the centroids and corners of the landmines which will in turn better help differentiate object boundaries.

Local Binary Pattern

LBP or Local Binary Pattern [76] is a useful Feature extraction Technique used to get texture based features like corners and edges. These variations are by their nature, non-uniform. There are various applications such as face detection. One of its characteristic working points is that is depends on the target's neighboring pixel. During the calculation, in LPB, a target pixels nearest 8 neighbors in all directions are considered. The target pixel is then compared to its neighbors. The comparison operator for a traditional LBP is the magnitude value. We will briefly discuss the workings and a figure illustrates the calculation process below.
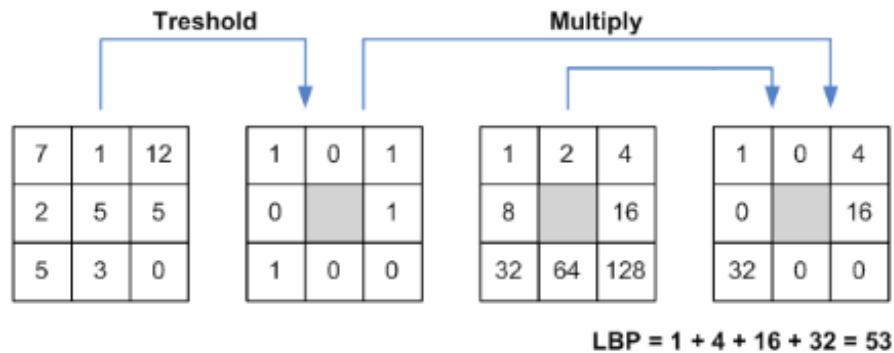

Figure 17: Calculating the LBP for the position show in grey.

In a more formal approach, we can assume to value at the central position to be g(c) and that of its 8 nearest neighbors to be g(p) . We then set the threshold s(x) such that the threshold s = 1 if x >= 0 else s = 0. The formula below then illustrates the process:

$$LBP = \sum_{n=0}^{7} s(g_c - g_p)2^n$$

In the calculation figure above, the pixel value in the grey position happens to be five. We begin with comparing it's magnitude with its 8 nearest neighbors and store the Boolean result of that comparison in another matrix at the position being compared thus e.g. as 7 is greater than 5 in the first position, in the comparison matrix we will store a 1 at 7's relative position in the input matrix. The position at 5 is greyed out as that's the value to be evaluated. Once all 8 comparisons a complete, we draw a magnitude matrix with values populated by power of 2 raised to n, where n is the position of the comparison i.e. as 7 was the first comparison, the binary matrix will have its first value as 2 power 0 or 1. The threshold matrix and the binary matrix are multiplied to give the weights which are used to compute histograms which can be thought of as feature vectors with 256 dimensions.

The kernel or the input window size 3x3 in the above case are arbitrary depending on the experiment but a few things are to be kept in mind. Kernels can extract more data around some particular regions than others. The stride or the jump of the kernel should be decided in such a way to introduce operational overlap so that no spatial information is lost. Non overlapping kernels will often lose information. Finally, for this project when calculating LBP features, it was decided to go for kernels of 10x10 and with an overlap of 50%.

Generalized Region Assigned to Binary

GRAB[77] or Generalized Region Assigned to Binary is a "generalized" variant of the LBP discussed previously. It's primary advantage being invariant to scale. The LBP was already invariant to some transformations like rotation, translation and illumination but if the image was scaled, then LBP directly operating pixels with their neighbors would suffer. GRAB solved the problem by not manipulating the central pixel with its 8 nearest neighbors in the same window. It extracts features from multiple scales of the image by using a "pyramid" like arrangement. The workings are explained below.

GRAB begins with normalizing the image which is simpler terms can be thought of as contrast enhancement, one way to archive this is histogram equalization discussed previously. This is followed by applying an averaging kernel over the image to "smooth" it. The averaging filter with a kernel size of NxN e.g. 3x3, 5x5, etc. passes over the image with jumps or strides and assigns the central pixel in each region an average based on the values of all neighbors. Once both these operations are complete GRAB applies LBP neighboring operation over the image. For this project, we applied the averaging kernel thrice with kernels of 3x3, 5x5 and 7x7, following up with a Uniform LBP neighboring operation to extract the features.
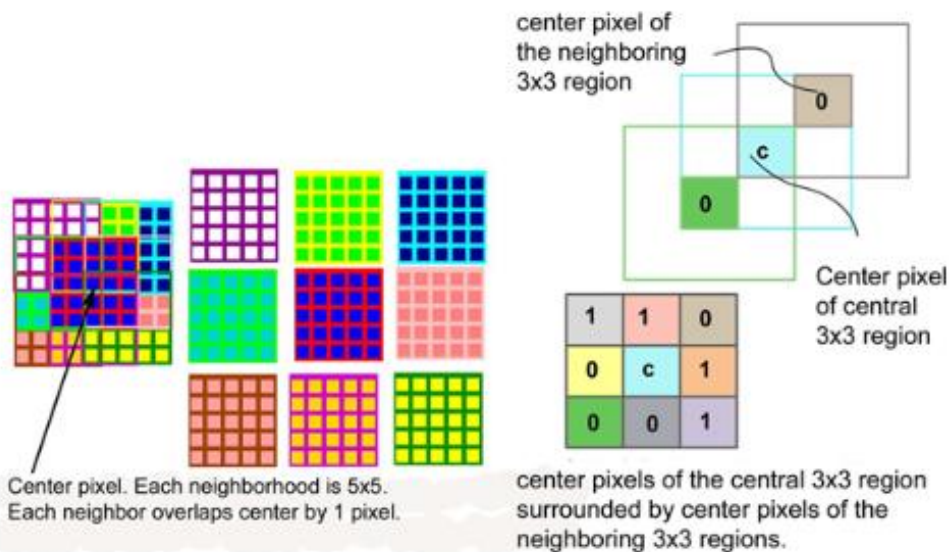

Figure 18: GRAB feature extraction technique taken from the original paper.

35

The above figure shows the image firstly being smoothed using a filter kernel followed by applying a LBP neighborhood operator. The central pixel is compared with its neighbors and a threshold is applied, the image is broken into multiple local regions and then GRAB histograms are evaluated. A primary observation being that this time the comparison is not one within the same window pixels but there are multiple overlapping windows as shown with the blue window in the middle in the figure having 4 neighboring windows of 5x5 with overlaps with the central window being 1 pixel.
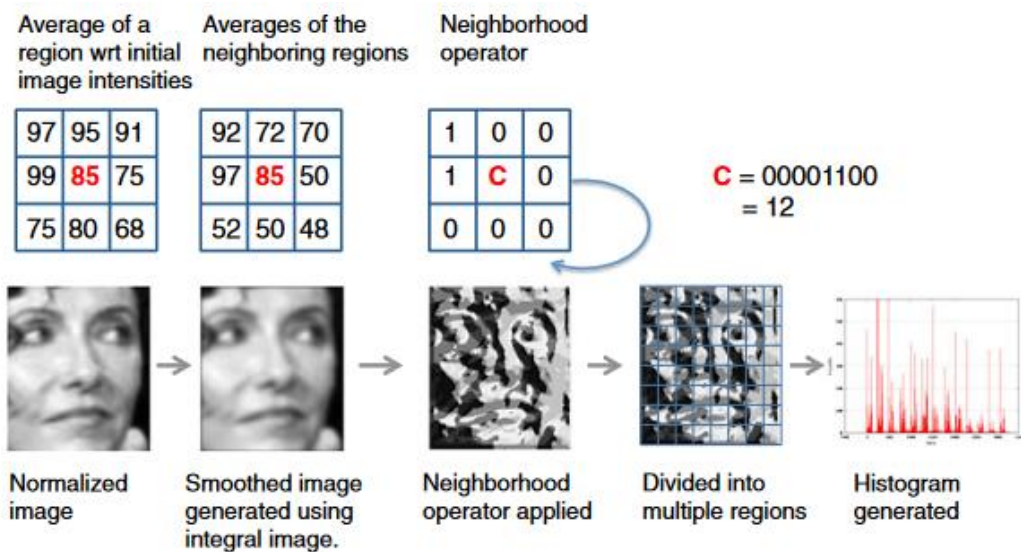

Figure 19: GRAB pipeline illustrating the process step by step.

Histogram of Oriented Gradients

HOG or Histogram of Oriented Gradients is a feature description technique used in Image Processing for object detection problems. HOG counts the number of occurrences of gradient orientation within small localized chunks of the image, filter kernel or a region of Interest. This technique got popular after Bill Triggs and Navneet Dalal published a groundbreaking paper in CVPR 2005 [78]. HOG used to be the State of the art technique for object detection before Deep Learning. It is specially known for being used in pedestrian detection problem.

In HOG, the histogram illustrates a distribution of the gradient directions (orientations) that are used as features. The gradients themselves are useful as they have large values around edges and discontinuities in an image. HOG works with a block which is simply a sliding kernel in which the gradient magnitude and orientation (Horizontal and Vertical gradients) are computed by applying 1D horizontal and vertical discrete gradient masks as follows:

$$([-1, 0, 1]^T) \, , \, ([-1, 0, 1])$$

Image is then divided into 2x2 cell grid and HOG is computed for every NxN chunk e.g. 8x8. For each chunk the gradient vectors are then quantized into bins so basically we are plotting a histogram of gradient magnitudes and angles we just computed so the x axis is angles and binned into 9 bins each with 20 degrees. Observing an 8x8 patch and having computed the Magnitude and Orientation, a bin is chosen based on the orientation and the value to be put into the bin/vote is chosen based on the magnitude. It is also important during implementation to remove redundant pixels from the image.
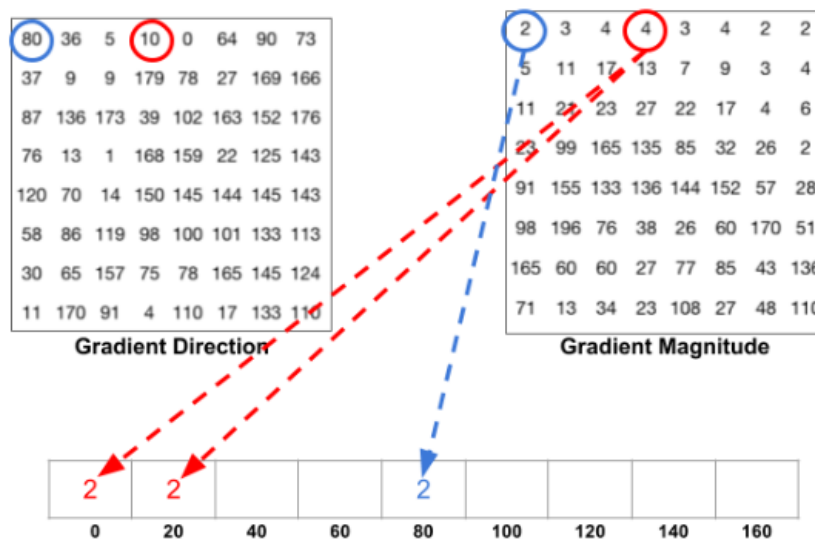

Figure 20: Histogram Computation in HOG

The figure above shows a Histogram of 9 bins being computed. The circle in blue shows a pixel with a direction of 80 degrees and magnitude of 2, thus adding 2 to the 5th bin. The red pixel has an angle of 10 with a magnitude of 4, since 10 is halfway between the 0 and 20 bins, 2 is added to both bins as the vote is evenly split. We implemented the binning process (bi-linear interpolation) to prevent the effect of aliasing.

Having computed the histogram of gradients for the image, we run into a problem. Gradients are very sensitive to lighting in the image, if we choose to make an image dark by dividing all image pixels by 2, the gradient magnitudes will change by half, halving our histogram values. To make the histogram independent of lighting conditions, we "normalize" it. Assuming an RGB pixel vector of [128, 64, 32]. We can compute the length of this vector as:

$$\sqrt{128^2 + 64^2 + 32^2} = 146.64$$

The length is also known as the L2 norm. If we now divide each vector element with 146.64, we normalize it to [0.87, 0.43, 0.22]. We can observe that we have removed the "scaling" in effect making it invariant to lighting differences. In the context of the thesis, we used the L1 norm, so for a vector X: [3,4], the L1 norm will be as follows:

$$||X||_1 = |3| + |4| = 7$$

Now we can normalize our 8x1 histogram as the 3x1 vector in the example. But a better idea is to normalize it over an NxN cell block such as 8x8, forming a 36x1 feature vector. This has 2 primary advantages, the low contrast regions within the block are enhanced. Secondly by normalizing within overlapping blocks no spatial information is lost.
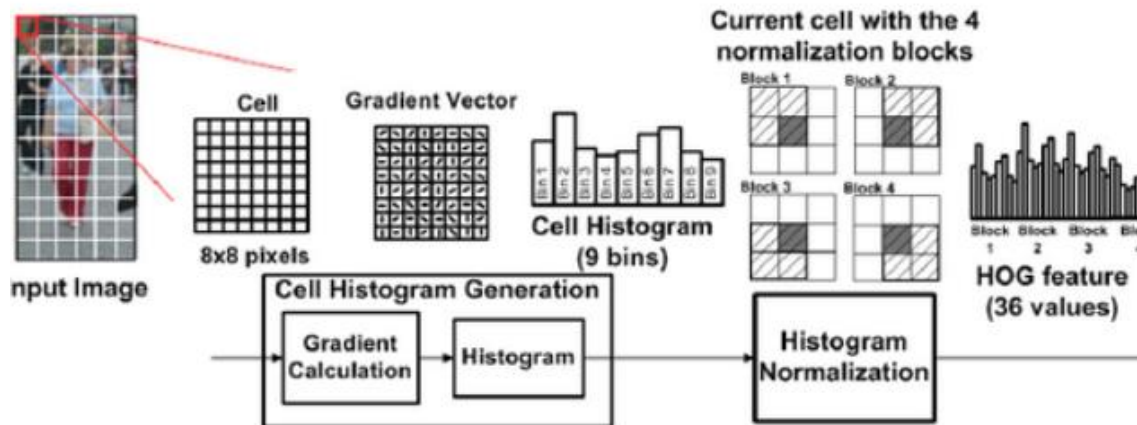

Figure 21: HOG pipeline.

Local Energy based Shape Histogram

LESH [79] is a feature extraction algorithm employed to get information of an image object's shape. It converts the image into a group of local energies in different kernel orientations based on feature perception. It also computes many local histograms on small patches of the image and concatenates them into a 128 dimension spatial one. LESH is designed to be scale invariant. It starts by dividing the image into 16 patches and every patch is convolved/passed with a bank of Logarithmic Gabor filters in 5 different scales and 8 orientations suggested for best performance [80], these detect mostly lower level features invariant to scale, lighting and contrast. Filter Bands are an array of kernels that break the input image into many components, this process is called analysis and conversely, the reconstruction process is called synthesis. The parameters such as filter bandwidth, orientations and scales depend on the scenario.

Energy values are computed and normalized for every chosen orientation and along all 5 scales. Along pixel positions, these energy values are compared and a Label map is calculated for

orientations with largest values. Finally for all 16 patches, 8 bin histograms are computed and merged to provide the 128 dimension spatial histogram. Another reason to concatenate the histograms comes from the fact that this preserves the relation between different image regions.

The local histograms are computed as follows:

$$h_{r,b} = \sum W_r \times PC_2(z) \times \delta_{r-b}$$

$$W_r = \frac{1}{\sqrt{2\pi\sigma}} e^{[(x-r_{x0})^2 + (y-r_{y0})^2]/\sigma^2}$$

Here W is the Gaussian weighting for a region (r) within the image (z). PC represents the local energy for the region and delta represents the current bin and the kronecker's delta for the label map L [80]. From an implementation POV, we used FFT (Fast Fourier transform) to implement the convolutions. The specification of the filters in frequency domain was done using parameters. The Gabor Convolution returned an EO, a 2D cell array with complex value convolution results as

EO{s,o} = convolution result for scale s and orientation o.

The real part represents the result of convolving with an even symmetric filter, the imaginary part from convolution with an odd symmetric filter. The implementation worked on all arbitrary size images but was fastest for images cropped to squares with sizes that were power of 2.

Local Phase Quantization

LPQ is a robust feature extraction technique that focuses on texture classification and computes feature descriptors invariant to image blur [81]. It locally computes phase information for all windows in the image. For the 4 low frequency components, phase values are computed, de-correlated and quantized into 8 dimension space. For the 8 dimension encodings, histograms are computed and concatenated, these are our feature vectors.

LPQ also calculates STFT or Short Term Fourier Transforms in rectangle neighborhoods/patches for all pixels. We take all complex coefficients that correspond to 2-D frequencies. For every position of the image window, we calculate covariance matrices with L2 norm between corresponding points. The covariant coefficients are de-correlated. If the samples are statistically independent, scalar quantization preserves data. We can achieve statistical independence by applying whitening transformation at all window positions. For every pixel position in the image window, quantization can be performed using a scalar quantizer. Quantized values are integers in the range 0-255 written in binary codes. Finally, the 256 bin histogram of these binary integers of the image is computed as our feature vector.

From an implementation POV, we computed a short term Fourier transform for each block. For de-correlation, we used SVD (singular value decomposition) with C (covariance matrix) and the transformation matrix M as SVD(D) where D = M * C * M';

After the quantization of values the result matrix F was passed through a whitening transform using the vector V from the SVD operation and the values were binary coded to 8 bit integers.

Weber Local Descriptor

WLD [82] is a simple but powerful local feature/texture descriptor. It is inspired by Weber's psychological Law which states that a change in stimulus will be barely noticed if it is a constant ratio of the stimulus. If a change in the stimulus is smaller than this ratio, a human observer will classify it as a background noise rather than an observation. Based on this law, the WLD is calculated based on two observations. Firstly the intensity of the current pixel (pixel orientation) and secondly, the relative intensity differences between this current pixel and its neighbors (differential excitation).

$$
\begin{aligned}
&\xi(I_c) = \arctan\left[\sum_{i=0}^{p-1}\left(\frac{I_i - I_c}{I_c}\right)\right] \\
&\theta(I_c) = median(\theta_i) \quad (i=0,1,\ldots,p\text{-}1) \\
&\qquad \theta_i = \arctan\left(\frac{I_{R(i+4)} - I_i}{I_{R(i+6)} - I_{R(i+2)}}\right) \\
&R(x) = mod(x, p)
\end{aligned}
$$

Figure 22: Computing WLD feature for a pixel

The figure above shows how to compute a pixel's differential excitation (ξ) and orientation (θ). The excitation equation is computed by computing differences of the pixel's neighbors with a center point, applying webers law over all neighbors and summing them. The arctan filter is applied for robustness to noise.

$$ f_{diff}(I_i) = \Delta I_i = I_i - I_c. $$

$$ f_{ratio}(\Delta I_i) = \frac{\Delta I_i}{I_c}. $$

For the implementation within this project, we computed the differential excitation by convolving the image with kernels f1 and f2 and mapping the ratios into [−π/2, π/2] range. Similarly, we computed the orientation by convolving the image with kernels f3 and f4 and matting the ratios into [−π/2, π/2] range. We quantized values into 8 orientations and

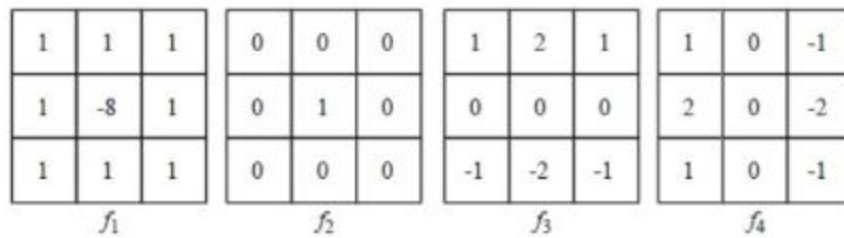computed the histogram of these values as our WLD feature vectors, the kernels are shown in the figure below.

1	1	1
1	-8	1
1	1	1

0	0	0
0	1	0
0	0	0

1	2	1
0	0	0
-1	-2	-1

1	0	-1
2	0	-2
1	0	-1

f_1 f_2 f_3 f_4

Figure 23: Kernels for the WLD.

3.4   Classification Techniques and Architectures

The performance of applied techniques in any previous stages as well as this phase will define the results of the classification and the success of this project. The phase of target classification can be thought of as a graphical image based signature identification where pixels within the image are grouped between target/non-target classes an example being noise/clutter and AP mines. In a more theoretical manner, all classification techniques are grouped into 2 main categories. Supervised classification where we have pre-hand information about our target objects and we use labelled training data or truth values to help our model train in identifying that particular object for example. Unsupervised classifiers are primarily based on the concept on clustering pixels based on similar visual properties e.g. an edge, same color, contrast etc. without any pre-hand knowledge or labelled training data. The methods with which classifiers compute their classification on image pixels and their context is of importance. We can have four main scopes in classifiers [83]:

- Per pixel classification
- Sub pixel classification
- Per-field classification
- Knowledge/Information based classification

In our case, being landmine identification, supervised classifiers may be employed in the case where there is available information about the landmines/target object present in the data such as their type or where the case is that a specific type of landmine is present but it's IR spectral signature is not known. Un-supervised techniques do not automatically yield good results in all possible random scenarios and also unfortunately suffer for huge FARs (false alarm rates) because of small number of target object pixels against background clutter. Thus while unsupervised classification may be useful to detect a new or unknown landmine in newly collected data. It is in our case, partly a necessity to employ supervised classification to identify mines as we will see in later sections.

Before we move on to the next phase of experimentation and results, we feel it necessary to acquaint the user with some information of the classification techniques that we employed or ones that were valid choices in the context of this project so that the user will appreciate their employment in the coming sections.

K means clusters

This is a highly popular unsupervised clustering techniques available to multi-spectral data. Its working principle being that image pixels be clustered/grouped based on their graphical similarity. To start the process, k centroids are randomly computed & deployed. Following which every pixel in the image is grouped to the centroid nearest to it. The method to compute the distance between this pixel and its centroid is up to the users, some of the valid choices are standard Euclidian, Manhattan, maximal distancing or a hybrid of these. Next new centroids are computed based on the mean of the pixels in each cluster and clusters are remade based on these new centroids and the pixels nearest to them. This method is looped until the number of epochs are reached or classification distances are minimized/stabilized i.e. next cluster will be almost identical to current one [84].
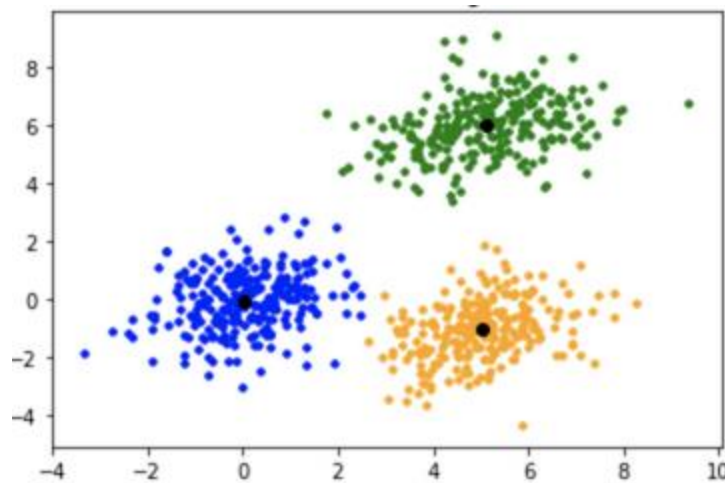

Figure 24: K means clustering with 3 centroids (black dots) and their clusters.

Support Vector Machines (SVM)

This is one of the simplest supervised classifiers. It was introduced for regression and binary classification scenarios [85]. Currently it is often employed for hyper spectral classification [86]. The working principle being drawing the best possible boundary/separator line between two classes. The training classes are known as support vectors and the boundary computed to separate them are called hyper-planes. One of its best advantages is that it is immune to the Hughes effect i.e. curse of dimensionality where the performance of the classifier starts to drop

as complexity note dimensionality increases. Another reason to consider SVMs is that even if the amount of available data is very small and/or the means of the classes is very close, separation is still possible [87]. The working is explained as follows:
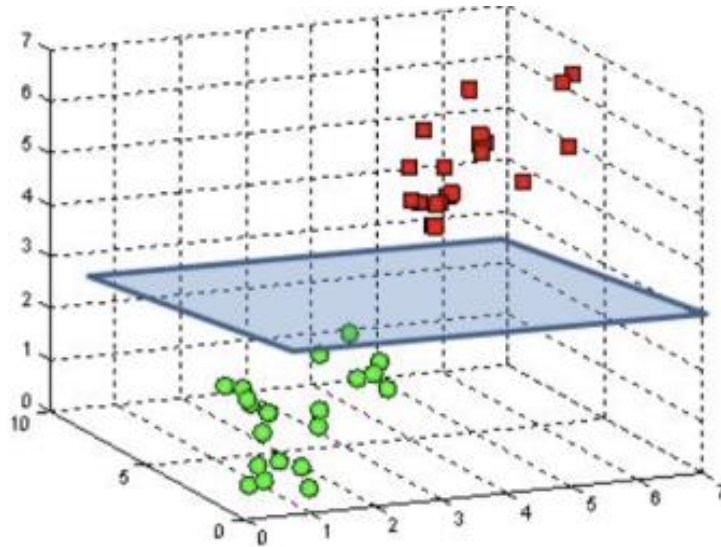

Figure 25: SVM illustrated with 2 classes and a hyper-plane separating them.

We introduce our training classes of the form (x,y) where x is a n-dimension vector representing the spectrum to which the pixel belongs where n is the number of channels/wavelengths of the hyper-spectral image. y is the class label representing the class of the pixel within the image as is in the range of -1 to 1. If the classes are linearly separable, the hyper plane is computer and represented by a mathematical function f(x) = w(x) + b. Where w is the vector component and b is the bias required to evaluate a boundary between two classes with no errors. In cases where two sample classes cannot be linearly separable, we can employ kernels for projecting our classes onto a higher dimension space where they can be linearly separated by a hyper plane. We keep in mind that projection will require a transformation where the inner product will be modified with a constant as the two equations below illustrate:

$$\left(x_i . x_j\right):$$

$$k\left(x_i . x_j\right).$$

We can choose between many kernels such as:

Polynomial kernels:
$$K(xi, xj) = (1 + xi.xj)^q$$

Sigmoidal kernels:
$$K(xi, xj) = \tanh(\alpha_0(xi.xj) + \sigma^2)$$

When multiple classes are to be classified (>2). There are two possible approaches. We can work with the 1 against everyone or 1vN case where one class is discriminated against samples of all other classes or we can use an arena 1v1 which as the name suggests compares 2 sample classes at a time from a large sample space.

Multiple Layer Perceptrons (MLP)

MLPs are a class of simpler neural networks based on the concept of feed forward and feedback. They comprise of 3 layers of varying densities and lengths:

1. Input Layer
2. Hidden Layer
3. Output Layer

This 3 layer model allows it to represent and map non-linear problems [88]. As stated above each layer can have any number of sub layers or thicknesses which may in turn have any number of perceptrons [89]. An example is shown below.
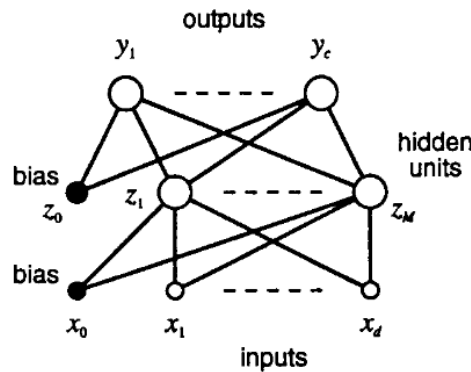
Figure 26: An MLP with 3 layers (horizontal layers)

The hidden layer has an activation function that is decided by the user such as linear, sigmoid, etc. A popular choice is sigmoid because the output is in the range of 0 to 1 and can easily mimic a probability distribution function. MLPs are trained with supervised learning and feedback/ back propagation minimizes the error function, its explanation is beyond the scope of this section.

Generalized Regression Neural Network (GRNN)

The GRNN are a class of one pass Machine learning algorithms with no back propagation. It performs relatively well even with small multi-dimensional datasets and the transitions between observations are very smooth. A neural network generally comprises of a number of interconnected but simple processors called neurons. They can compute in parallel and learn of given examples. In the given architecture diagram from the original paper [90] below, we can easily see that the Input layer is merely a distribution hub for the neurons in layer 2.
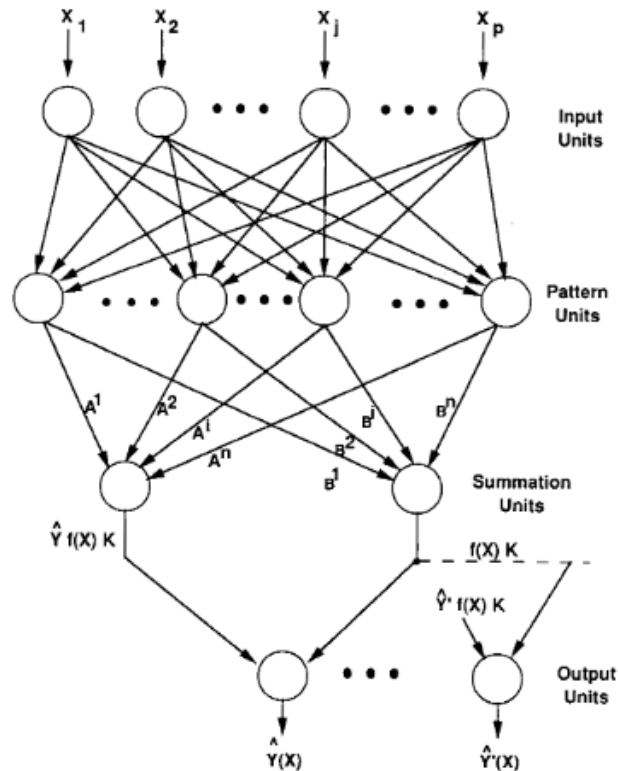

Figure 27: The GRNN block Architecture.

The model is based on the regression of Y, a dependent variable over X, being the independent variable. The model then computing the most likely value of Y for a given value of X based on a finite number of physical observations of X and the associated values of Y. Thus X being the system input and Y being the output. This model however does not assume that Y is a linear function of X, rather it computes a probability density function over the observations using parzen window technique [91] which is a reasonable choice for continuous density function. For a joint probability density function of Y and X, an expected value of the next Y can be estimated for the next value of X. Thus the architecture converges from examples instead of iterations. The output of Y being time dependent now on the propagation time through the architecture's 4 layers as seen above. A key requirement of this model however, is the need to scale the inputs

until they have roughly the same variances. This requirement is based on the fact that the pdf will be evaluated over the kernel/window with the same width for every dimension.

The simplified workings are as follows:

- The architecture relies on the given two vector pairs (Xi,Yi) and (Xj,Yj) where X is the Input Vector to the GRNN and Y is the vector to be estimated. The neurons in the architecture run in parallel and thus are not interactive. Not illustrated in the figure are the micro neurons that update the biases A and B between the Pattern and the Summation Layers and update the Cluster means in the Pattern Units. These Cluster means could also be updated using K means Clustering [92].

- For an Input Vector X passed into the Pattern Layer, a difference is calculated between X and the stored mean vector representation of each cluster, the difference is then passed on to the activation function which has a design requirement to be non-linear. A table of all possible activation functions can be found in the Table 1 of [93].

- The output of the Pattern Layer is then carried on to the Summation Layer. Here a dot product is performed between the weights vectors/weights and the output of the Pattern Layer. The output of this layer is in the form: f(X)K. Where K is a constant that can be estimated by the Parzen Window and is not dependent on the data. The output values are then multiplied with each value of Yj couples with the cluster mean Xi to obtain the output in the form Y.f(X)K. The output Layer finally simply divides the output of Summation Layer with f(X)K to yield Y.

The primary advantages to using GRNN are faster training times and convergence to best fit regression surface. It is especially useful with real time use cases with sparse data. It also does not rely on back propagation which requires long training times [94]. Back propagation models also have the problems of converging to local minima instead of the global minima. A key disadvantage of this technique is that the deployed (trained) system generates outputs slowly because of the large amount of calculations required [95]. A more keen reader can explore the theory of probabilistic neural networks for a better understanding of GRNNs [96].

Chapter 4

This chapter discusses the results and analysis of various approaches and algorithms that run on the preprocessed data which consists of Spectral Signatures that were reflected back from the soil by a mine or a clutter object. We will observe the implementations of feature extractions and classification by various machine learning approaches described in the previous chapter in an effort to compare them. We shall observe that feature sets belonging to spatial and shape orientations are the primary contributors as opposed to surface and textural feature sets.

A careful examination of the data will show that it is made up of alternating signatures of mine and non-mine objects and as with each have various unique patterns that can be exploited by the feature extracting techniques. Moving on, the Machine Learning techniques will classify the input signatures into mine and Non-Mine/Clutter/Noise. We shall discuss several feature extracting techniques such as Histogram of Oriented Gradients, Local-Binary-Patterns, etc. The Data Classification techniques under discussion being Support Vector Machines and GRNNs. Finally we shall give a result based comparison and conclude the report.

To begin with, a major bottleneck in employing SVMs and GRNNs to testing and training is the lack of test data. This resulted in Linear SVM outperforming SVM-RBF (Radial Basis Function). For the testing and training phase, the data was chunked into ten equal chunks and 90% was used to training and the remaining 10% used for testing phase. This concept is known as 10 fold cross validation. The dataset is divided into 10 random parts and we used 9 parts for training and the tenth part to test. This procedure is repeated 10 times each time, the reserved testing part is changed. Our major reason to use this technique was to make sure the results obtained is a fair representation of the classifying algorithm's performance compared to say 2-3 fold CV (cross validations).

For this Project, we employed three operational datasets belonging to the Biometrics and Machine Learning Lab at the University of Florida. These are:

4. MPGSep2005
5. Small Millbrook
6. Tiny Millbrook

The first dataset comprises of 1791 images of while 496 are real landmine signatures. The Millbrook Datasets are compact datasets with 540 & 43 images. We conclude that Dataset 3 was too insignificant on its own to contribute to any major observations/results in the project.

4.1   Results Outline

In this section, we will outline the results obtained through combining various feature extracting and Classification Algorithms. We shall also observe that feature level fusion will aid the Net Accuracy in the Classification. We will finally discuss important observations that will aid to any future related work.

As mentioned earlier, a major bottleneck was the size of available data. The classification results of the Support Vector Machine-RBF does not perform as well as its linear counterpart. Thus the primary focus of this part will be the evaluation of the feature extraction Algorithms coupled with Linear SVMs and GRNN. To have consistency in data evaluation, the mentioned 10 chunk processing is followed. Results of coupling different FETs (Feature Extraction Techniques) and Classifiers is given in the tables in the coming sections.

Features	Feature-set size	MPGSept2005 (1791 samples)			Small_Millbrook (540 samples)			Tiny_Millbrook (43 samples)		
		SVM Linear	SVM-RBF	GRNN	SVM Linear	SVM-RBF	GRNN	SVM Linear	SVM-RBF	GRNN
HOG (8 bins)	1x7200	93.23	72.29	87.09	91.48	82.96	87.01	82.5	82.5	80
LBP (3 x 3 Window)	1x256	72.29	NA	69.83	76.11	NA	77.41	80	NA	75
LBP (10 x 10 window)	1x146944	77.97	72.29	75.52	85.18	82.96	80.90	82.5	82.5	77.5
ULBP (10 x 10 windows)	1x33866	76.7	72.29	68.71	84.81	82.96	73.7	82.5	82.5	85
GRAB-ULBP (10x10 windows)	1x101598	76.51	72.29	67.98	83.88	82.96	76.48	82.5	82.5	82.5
LESH	1x128	72.26	72.34	72.29	82.96	82.96	82.95	82.5	82.5	82.5
LPQ	1x24600	82.64	72.29	72.29	83.33	82.96	82.95	82.5	82.5	82.5
WLD	1x80	60.22	72.29	64.19	76.85	82.96	76.48	72.5	82.5	67.5

Feature Extractors	# features	MPGSept2005			Small Millbrook	
		SVM-Linear		GRNN	SVM-Linear	GRNN
		mean accuracy	±std dev	mean accuracy	mean accuracy	mean accuracy
WLD	1x80	60.22	±18.61	64.19	76.85	76.48
LESH	1x128	72.29	±18.60	72.29	82.96	82.96
GRAB	1x101598	76.59	±14.48	67.98	83.88	76.48
LBP	1x146944	78.04	±14.56	75.53	85.18	80.92
LPQ	1x24600	82.68	±11.96	72.29	83.33	82.96
HOG	1x7200	93.29	±5.24	87.09	91.48	87.03

Figure 28: Quantitative Comparisons of FETs and Classifiers.

The above table lists groups of Classifiers and FETs. We can see that for the MPG dataset, in case of all FETs, the Linear SVM Classifier beats the GRNN. As GRAB & LBP extract features mainly from the surface and texture of the image, while HOG and LPQ extract feature based on shape, we can see that shape based features were the primary source of distinguishing of Landmines and clutter based on far better accuracies achieved when using LPQ and HOG. WLD/LESH are on the other hand dependent on the angle and orientation of the object, the smaller number of features they extract result in inadequate classification results, thus confirming that classification results are highly dependent on the size of feature sets. For the case of MPG, the highest achieved Net Average Accuracy has been 93.23% by the HOG FET over Linear SVM Classifier. Moving on, the smaller Standard Deviation means that the features extracted by HOG finely discriminate the input image into the correct classes. In fact, if we compare all the FETs, HOG has the smallest Std. Deviation.

The Millbrook dataset is a smaller dataset than the MPG. But the results being consistent, HOG and SVM-Linear yield the highest accuracy while having the smallest Std. Deviation. For a better analysis of these observations, the following figure provides the Receiver Operating Characteristic Curves plotted for all the FETs. On the axis are the Genuine Acceptance Ratio and the False Acceptance Ratios. The perfect FET will have a GAR as high as possible with the lowest possible FAR. As the curves illustrate, the best performers were HOG followed by LPQ.
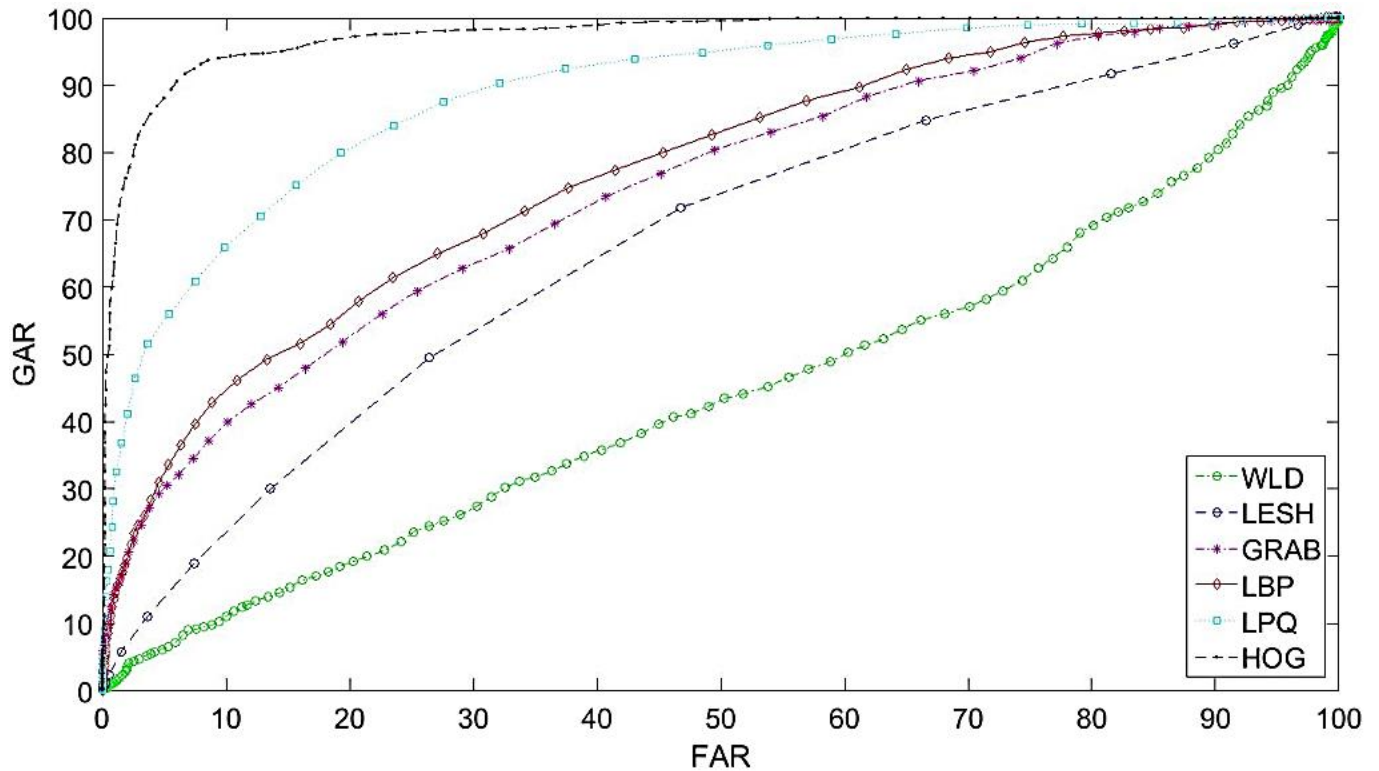
Figure 29: ROC curves illustration the performances of the FETs.

4.2   Feature Level Fusion

As we know that fusion can be had at many levels, fusion at feature level can be thought of as concatenating the features that different FETs extract. This theoretically provides us with the advantages of both algorithms. As illustrated previously HOG was the best performing FET. For this part, we will fuse HOG with other FETS and not the results using Linear SVM Classifier to have consistent results, note that the only changing variable is the FET being fused with HOG. In this project 2 fusion techniques were implemented, simple concatenation and Canonical Correlation Analysis (CCA), the techniques can be switched by commenting/uncommenting code lines.

| Feature Extracting Technique | No of Features | MPG2005Sep | |
		Net Avg Accuracy	Standard Deviation
HOG + LBP	1x15144	78.31	+/- 14.39
HOG + LESH	1x7328	93.22	+/- 5.28
HOG + LPQ + LESH	1x31928	93.89	+/- 5.63
HOG + LPQ	1x31800	93.95	+/- 5.52

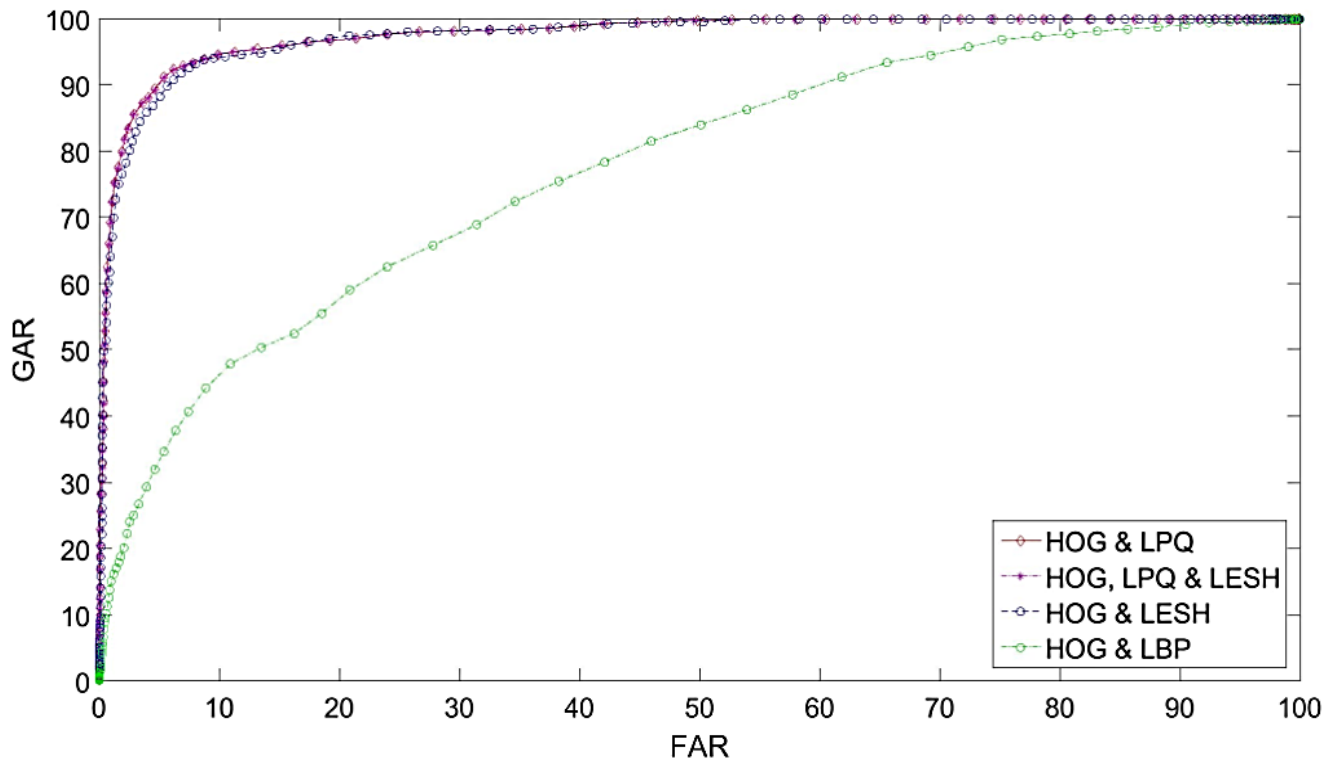Figure 30: Quantitative Comparison of Feature Fusion

Figure 31: ROC Curves for Feature Fusion.

The Table and the Figure above illustrate the results. Following the HOG, the 2nd best performing FET has been LPQ. We can observe that the fusion of HOG + LPQ features yield a Net Avg Accuracy of 93.95%. Moving on the fusion with LBP has not improved the results. While a fusion of HOG + LESH seems to provide some level of improvement, which may have to do with the increased size of the fused feature set. We can also observe that the fusion of HOG+LBP seem to be the least performing option. We will now provide the Illustrations for the Probability Density Distributions of FETs with respect to the similarity Scores arranged according to their accuracies.

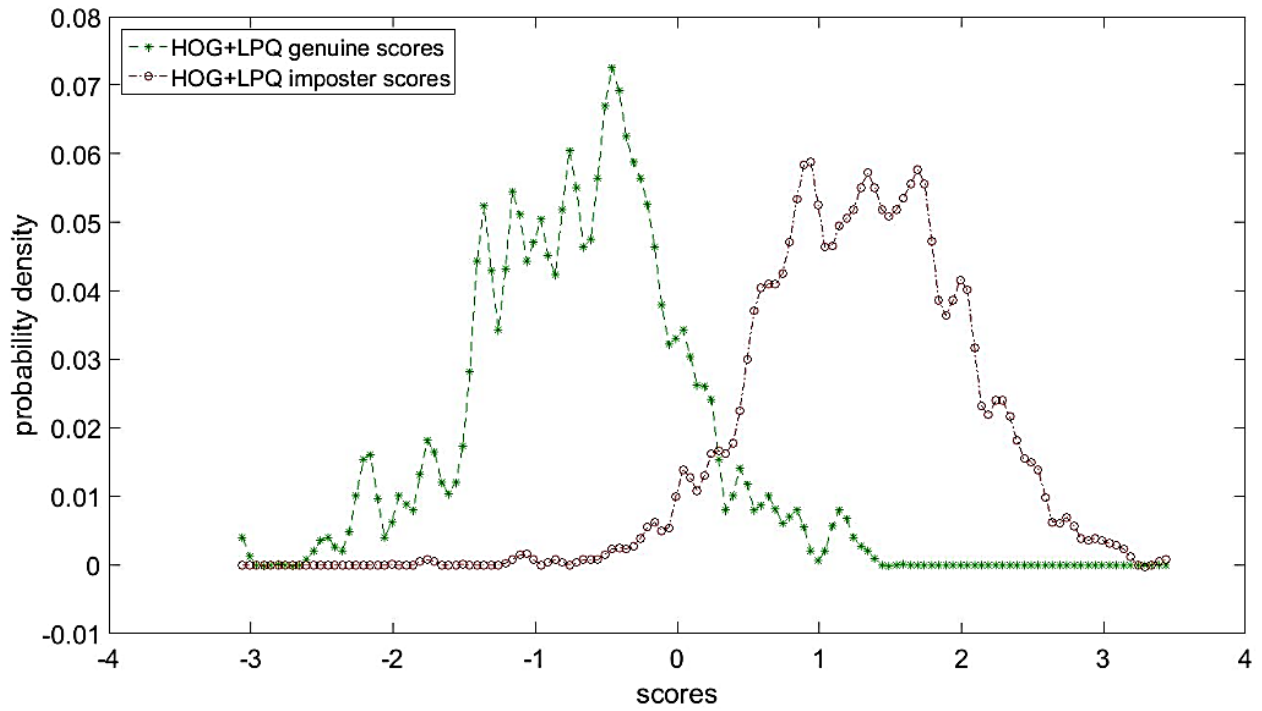## 4.3 Probability Density Distributions
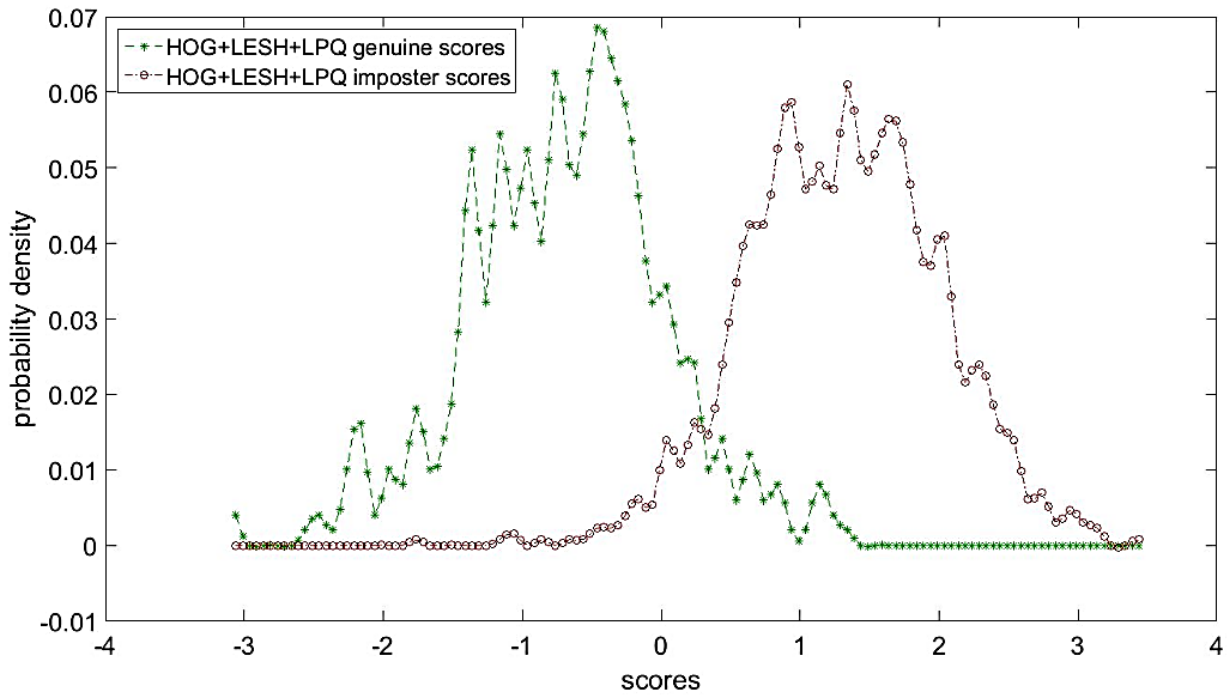

Figure 32: HOG + LPQ = 93.95%.
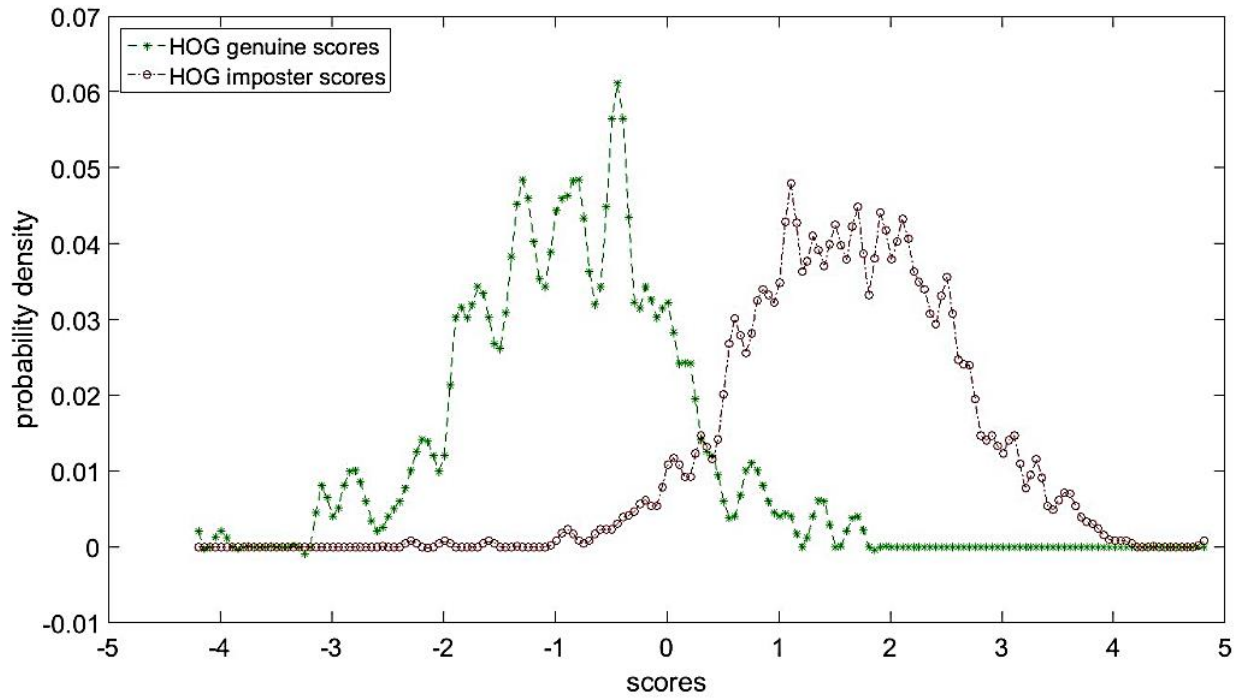

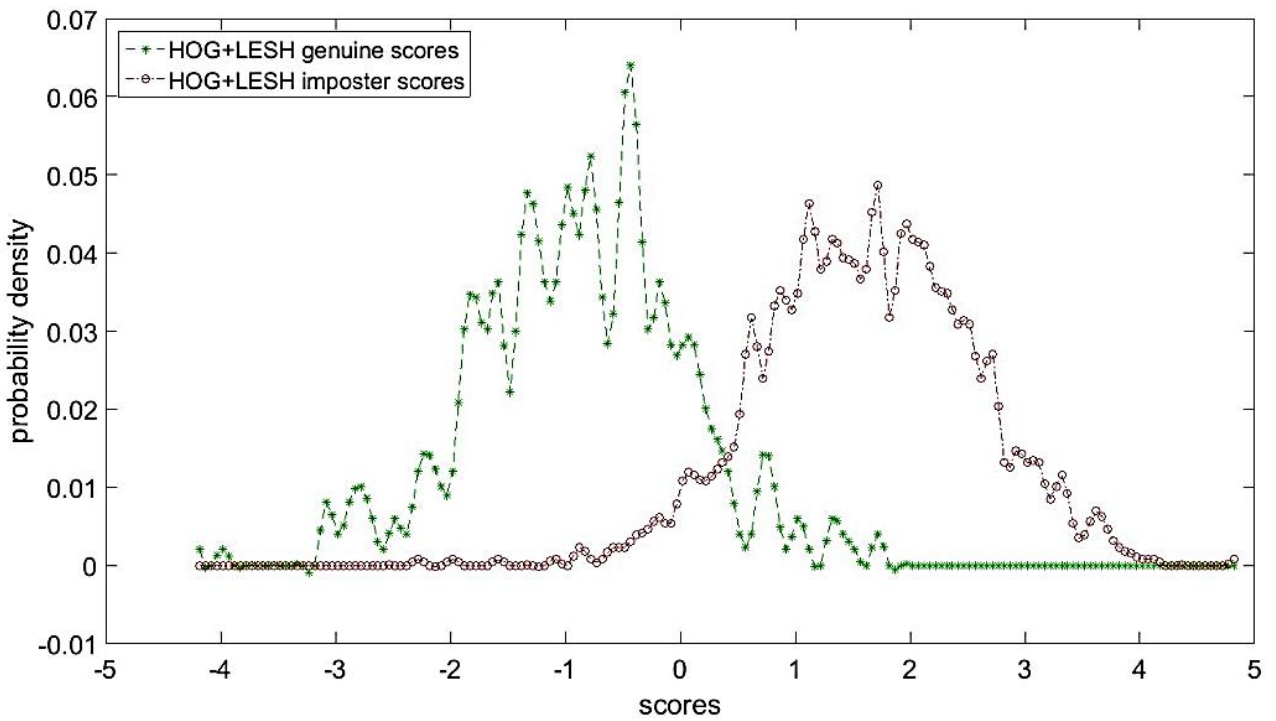Figure 33: HOG + LESH + LPQ = 93.89%

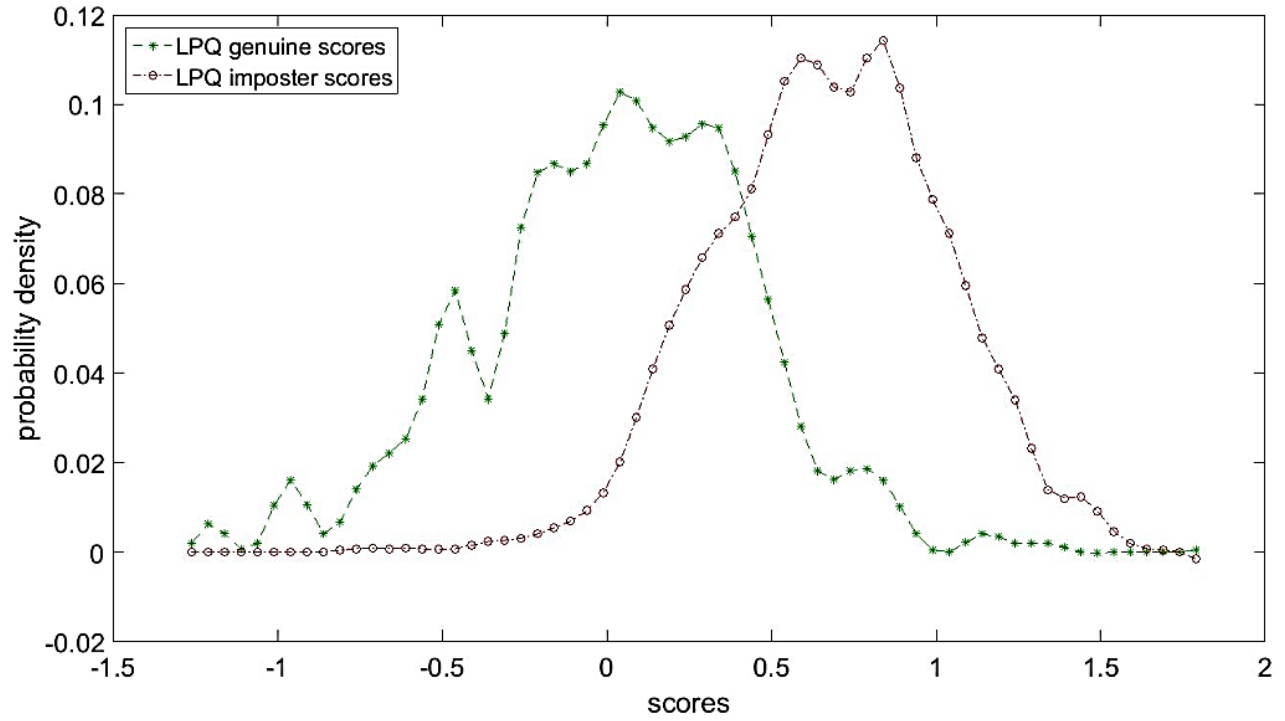Figure 34: HOG = 93.23%

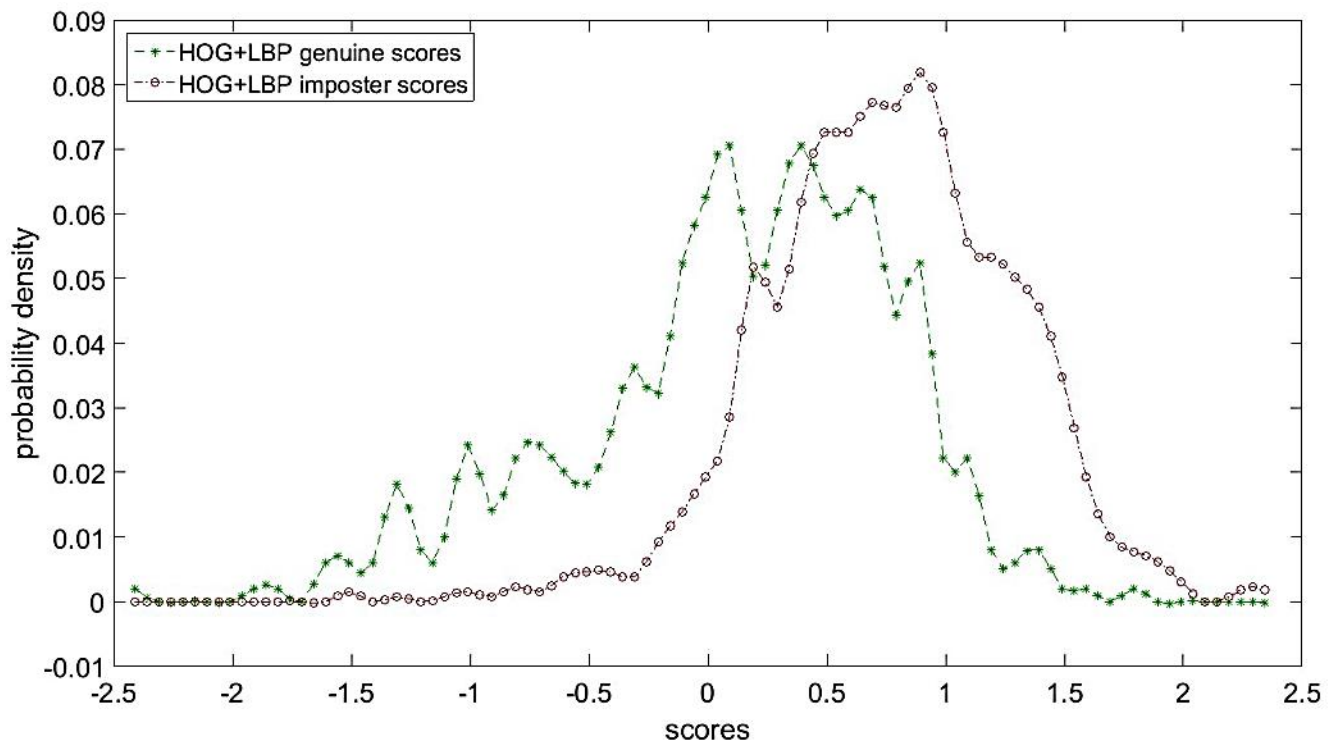Figure 35: HOG + LESH = 93.22%

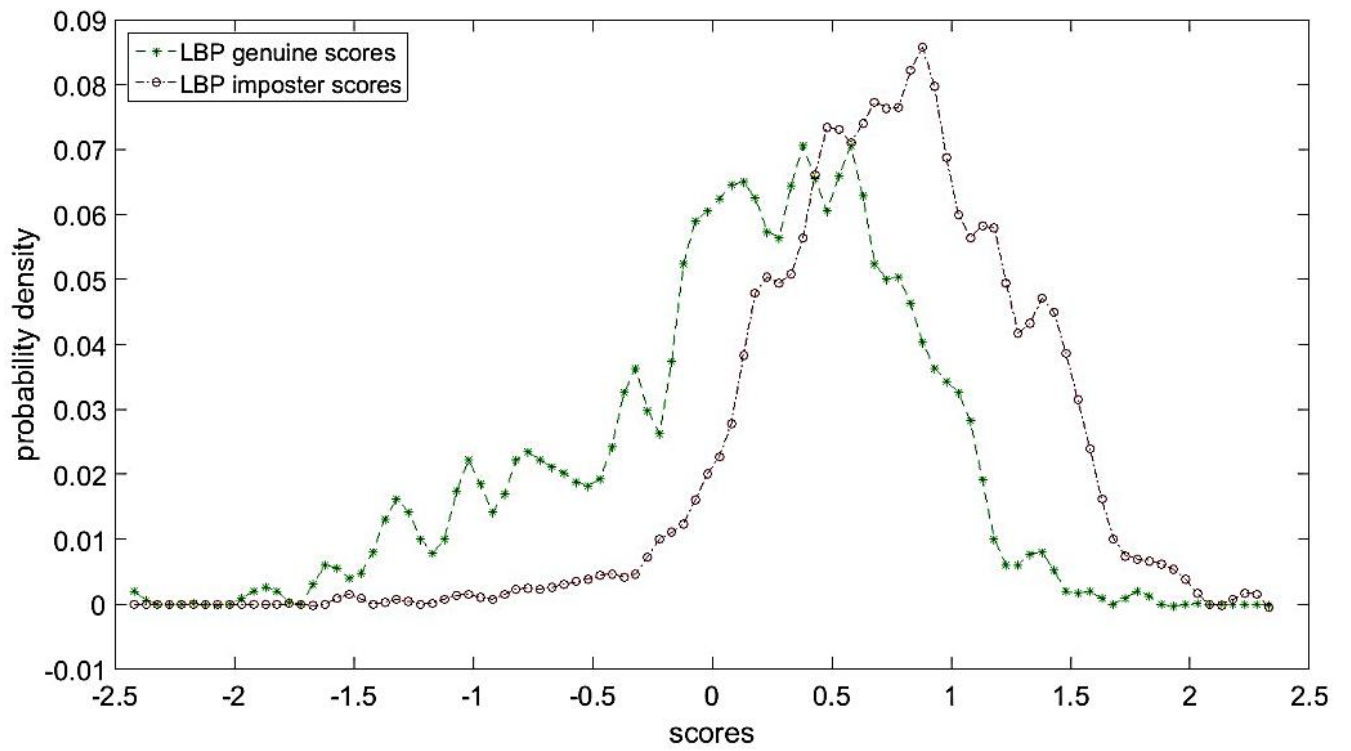Figure 36: LPQ = 82.64%

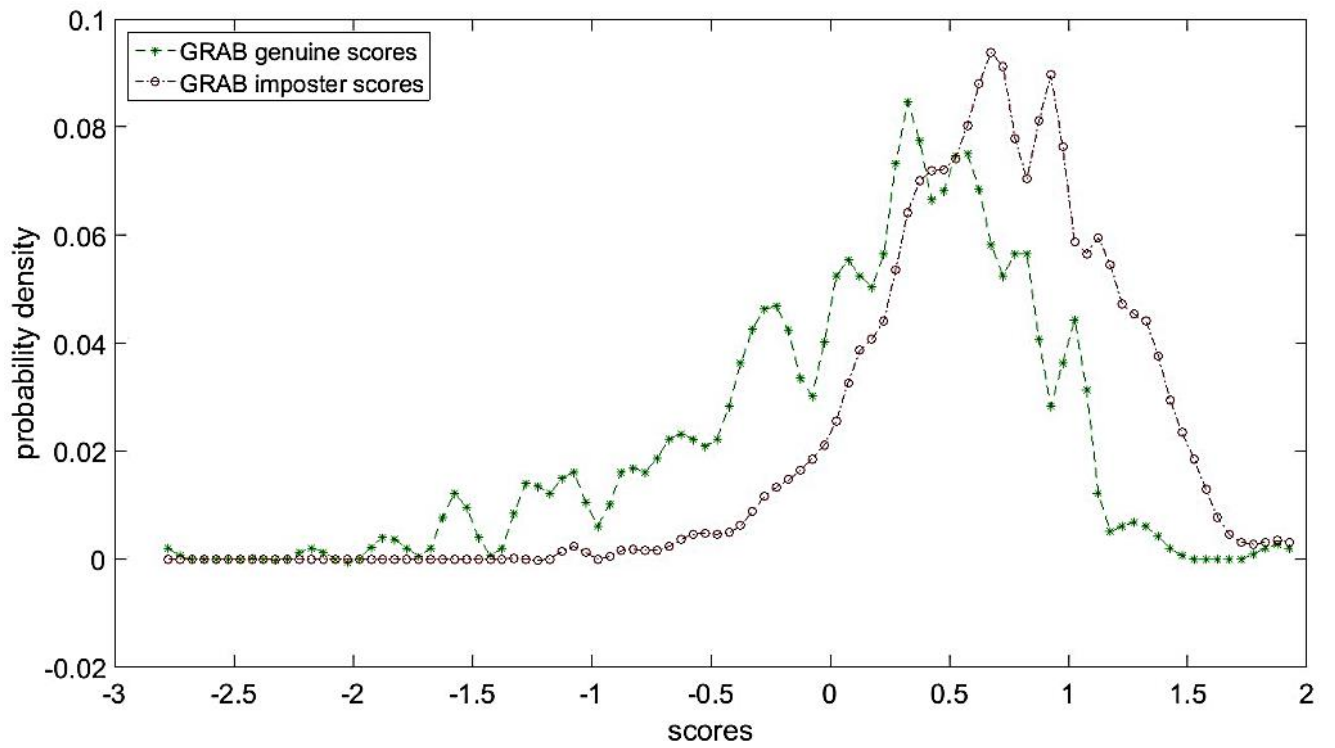Figure 37: HOG + LBP = 78.31%

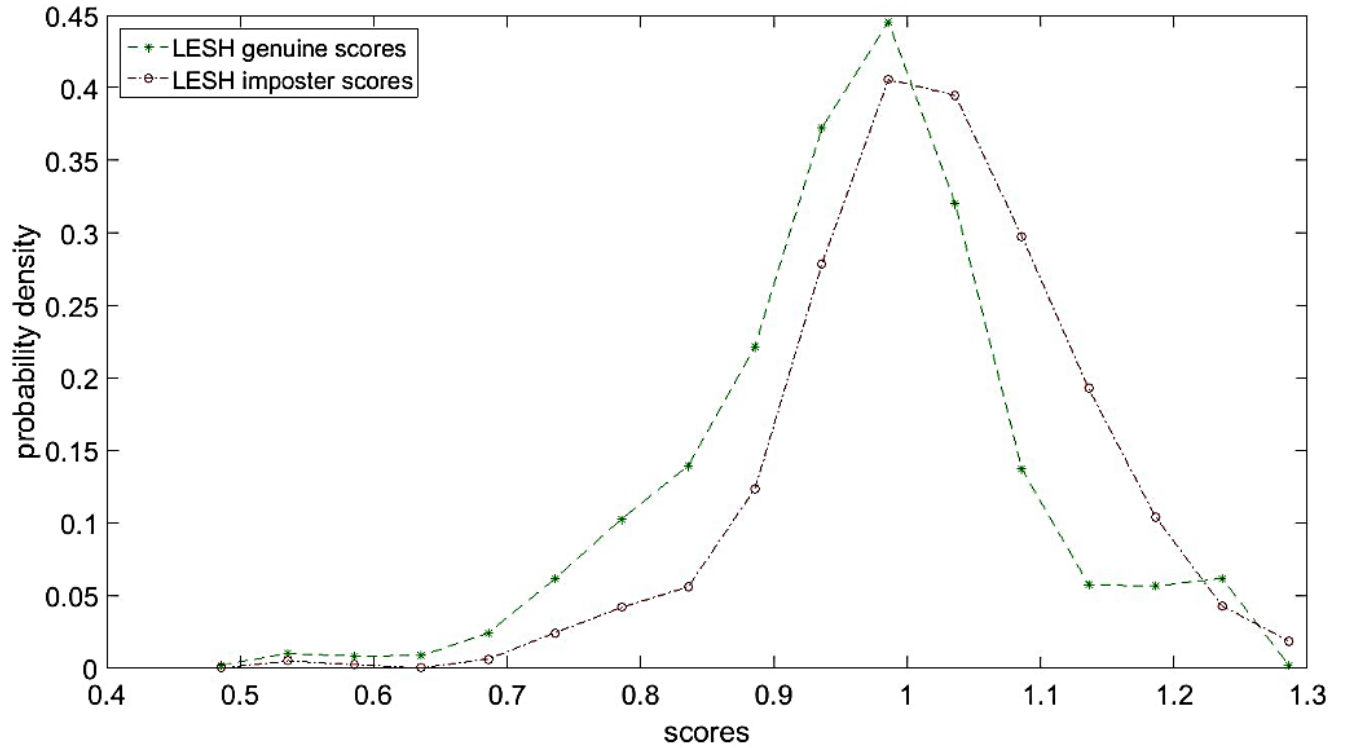Figure 38: LBP = 77.97%
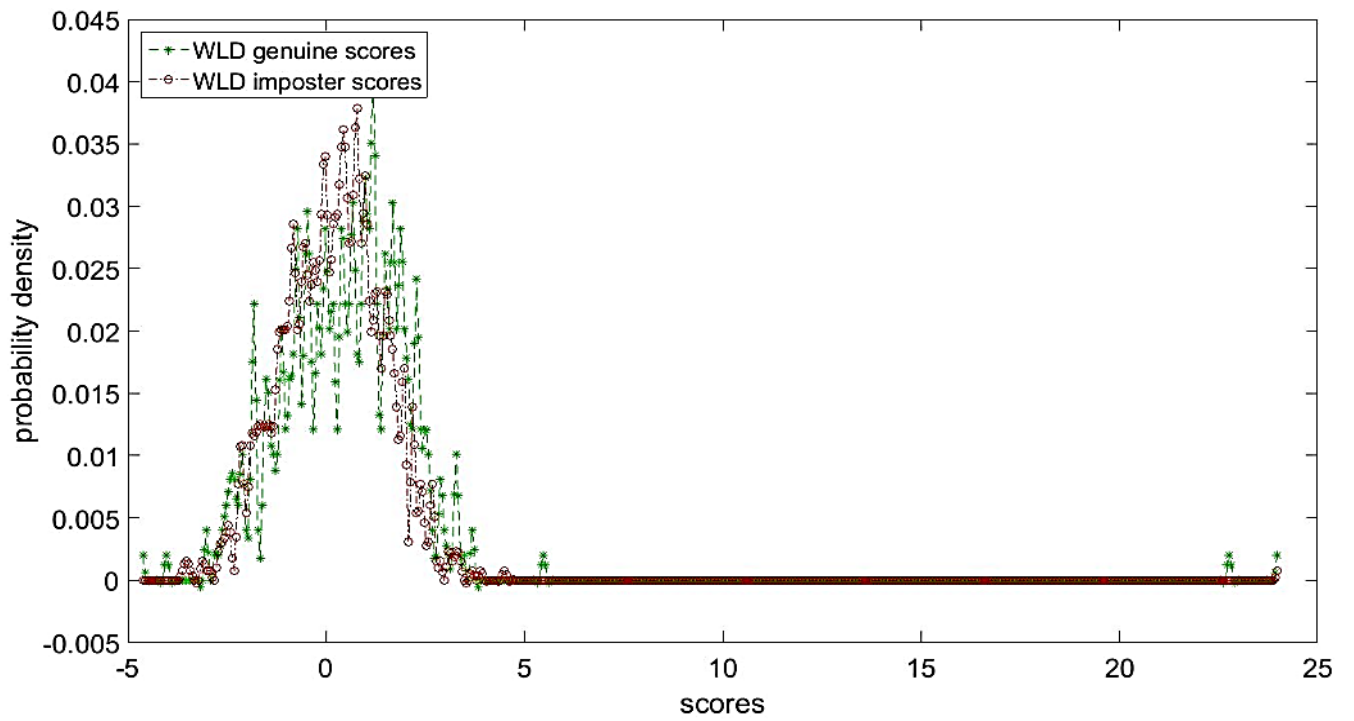

Figure 39: GRAB = 76.51%

Figure 40: LESH = 72.26%

Figure 41: WLD = 60.13%

4.4   Discussion

In this part we shall carefully observe the illustrations of Probability Density Curves and discuss the findings. The Linear SVM that was chosen for the curves output the scores that contained the posterior probability of the classes. In Statistics, Posterior Probability is a conditional probability P for any event A given that event B has already occurred. This comes from the adaptation of the Bayes Rule given below.

$$P(A \mid B) = P(B \mid A)P(A)/P(B).$$

As Bayes Rule is symmetric for both A and B with both conditional probabilities P(A|B) and P(B|A) calculable by readjusting the equation. The term "posterior" in that sense emphasizes then the probability we are inferring to, given that the other is known.

By considering one probability score, we can then consider the positive score values to be representing one category/class and negative scores to be representing the other. Thus we can segregate the inputs into genuine scores and imposter scores. For our project, we considered the genuine scores as Clutter/Non Mines Class and the imposter scores as the Mines Class. Plotting these two probability densities together gave us the figures above for each implementation. We would also mention that a smaller overlap between the curves is a sign of better performance. Thus it is now clear from the observations that the implementations with higher accuracies had less overlapping areas between the curves than those with lower accuracy. It can then be said that overlapping regions are directly proportional to class separability. The first 4 figures thus successfully separated and segregated inputs into the two classes as is observable with their smaller overlapping regions compared to other implementations.

A keener analysis of the other curves yield further observations. There must be a signature pattern in the image that itself is a proof of the class the image belongs to. As will be observable in the coming section, small batches of classification results are illustrated and it will be clear that because of the pre-processing involved among other factors, Non Mine signature images will have flatter signals symbolizing that they are similar to/blended into the background noise. The Mine signals on the other hand will have far more contrast. If the dataset used in the process was larger, it would have increased the accuracy as anomalies would not affect the scores that much. Also some of the FETs would have succeeded in decoding the exact patterns that are responsible for segregation inching close to 100% accuracy.

We can conclude the discussion by highlighting HOG to be the winning Feature Extraction Technique. While the workings of HOG are already discussed previously, the calculations of the gradient orientations form a thick grid with many overlapping regions. Input Signatures may have small spatial variations which are easily recognized by HOG. On the other hand LPQ is blur invariant, a strong advantage. Their fusion in the case of HOG + LPQ then succeeded in decoding the signatures belonging to the classes. We would also point out that employing feature

descriptors like SIFT key point descriptor would aid in decreasing the dimensions in input features.

4.5   Comparison and Discussion against CNN architectures

In order to have a meaningful discussion of our results, it would be best to include a discussion of a highly related and published piece of work to analyze our work with and to serve as a benchmark. We also felt that our results should be compared to a Convolution Neural Network or CNN based approach. The project under analysis [97] is a GPR or ground penetrating radar response/signature based and utilizes a CNN technique known as Auto encoders. The data is real and volumetric in nature, taken over landmine free regions with false objects inserted or placed over the terrain. It is an anomaly based detection approach where the project aims to recognize objects that do not "blend into" the terrain over several polarizations and thus are labelled as landmines. Its accuracy is close to 93% which is very close to what we achieved.

Since we are only interested in discussing the results and not in reviewing the literature nor how it works, we will summarize the novel aspects of the literature and provide links to its implementation. The concepts behind auto encoders as well as an in-depth analysis can be referred at [98]. A curious reader can also read up on implementation of auto encoders over geo-physical scenarios [99], [100].

- This is the only piece of literature implementing CNN over both vertical/horizontal polarizations.
- The project utilizes a full scale, military grade GPR capable to capturing 3-D response signatures rather than 2-D reflectance/absorption IR responses as in our case.
- This project implements a CNN based technique over a buried landmine detection problem which can be used in a cross dataset arrangement.
- Like in our case, this project is tailored to work with small datasets due to rarity of the data available.

The ideal approach towards the landmine problem is that we should always aim to detect 100% of the targets with as small amount of false negatives as possible. Where false negatives mean misclassifying a landmine as a clutter object/ non-explosive object. On the other hand, it is acceptable to have a high false positive ratio i.e. clutter objects misclassified as landmines also known as false alarms. To give a benchmark, United States Army accepts solutions with one false alarm at 1.25 meter square intervals [101]. As a matter of fact, no solution in the world has been able to fulfil the U.S. benchmark.

The pipeline of this literature is similar to ours which was discussed in Chapter 3. A common feature was the use of small volumetric chunks of data in their case and small chunks of 10 image blocks in our case, in both cases the motivation was similar.

- The splitting into smaller chunks with small overlaps allowed a larger volume of data for training, keeping in mind that real responses/signatures is expensive.

- More importantly, feeding the system with smaller chunks will allow lighter architectures to be used which performed better than their heavier counterpart e.g. SVM with Linear activation function beat SVM with RBF as the activation function.

- Thirdly, the use of chunks allows the whole pipeline to become independent of the size/amount of data as any arbitrary number of equally sized chunks may be used.

We now briefly discuss the acquisition system used in their case and firsthand see the similarities in the properties of spectral signatures. The Ground penetrating Radar used in their case is an IDS Aladdin model with an impulse module carrying dipole antennas with a base frequency with a bandwidth around it comprising of 2 Ghz. The dipole antenna pair are configured for orthogonally polarized scanning.

The authors also used multiple datasets in different terrains but acquired using the same equipment and targets. They included use of 2 sandpits of 1 meter and 2 meters with the targets buried in range of 5 to 15 centimeters. The details are available below.

Parameter	S_1	S_2
Central frequency / Bandwidth	2 GHz / 2 GHz	2 GHz / 2 GHz
Propagation velocity in soil	14 cm/ns	10 cm/ns
Time sampling	0.0117 ns	0.0117 ns
Inline sampling	0.4 cm	0.4 cm
Crossline sampling	0.8 cm	1.6 cm
Time window	15 ns	20 ns
Number of acquired B-scans (Y)	114	66

Lastly, before we move onto the performances, evaluation metrics and results, we would like to point out how similar the spectral signatures perform wether in 2-D scans or 3-D volumes. The figure below illustrates the concept, the second strip with landmine objects have distinct peaks that are clearly visible despite the landmines being camouflaged/buried into foliage.
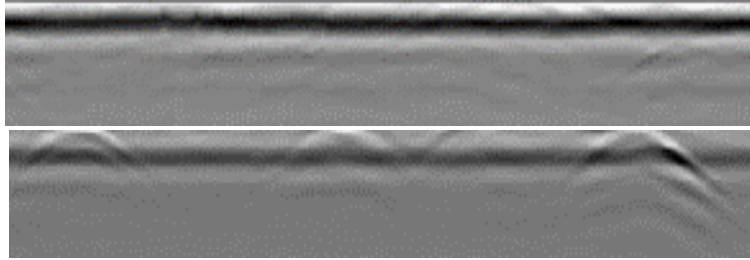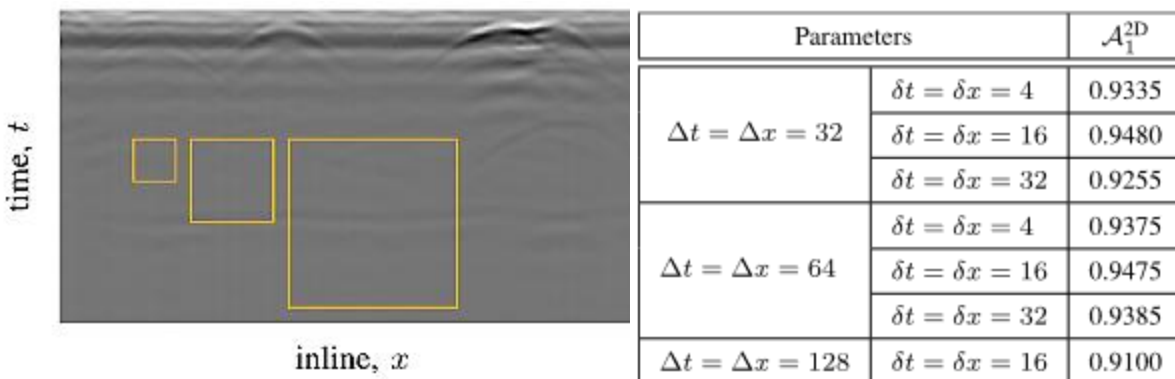
Figure 42: 3-D signature responses from a GPR, the first strip is unmined (no targets), the second strip is mined.

In both projects, the techniques are evaluated using ROC or receiver operating characteristic curves. These curves symbolize the conditional probability of correct detection (landmine) against the probability of false alarms (detecting a landmine in a mine-free image/sample) by plotting all possible values of the probability variable/threshold. As a good estimate of the performance, the area under the ROC curves was selected. This gives us a good estimate of where the technique stands in terms of overall performance. This will lie between the range of 0 (inverted result, opposite of the truth value every time), 0.5 (random estimate or guessing) and 1 (perfect estimation).

As we are interested in the 2-D results of the works which are a good rival to ours, we will not be comparing the 3-D results. One of the first discussion should be on Block size and stride being the first hyper parameter. A strip figure below shows an arbitrary sample with varying block sizes of 32, 64 and 128 samples. A good observation here is that smaller strides will symbolize more overlap. This will make the feature mask a lot smoother and thus is desirable than larger block sizes but it will also require more memory usage in terms of training and testing as there are more "patches" to analyze.

Parameters		$\mathcal{A}_1^{2D}$
$\Delta t = \Delta x = 32$	$\delta t = \delta x = 4$	0.9335
	$\delta t = \delta x = 16$	0.9480
	$\delta t = \delta x = 32$	0.9255
$\Delta t = \Delta x = 64$	$\delta t = \delta x = 4$	0.9375
	$\delta t = \delta x = 16$	0.9475
	$\delta t = \delta x = 32$	0.9385
$\Delta t = \Delta x = 128$	$\delta t = \delta x = 16$	0.9100

Figures 43 & 44: Zoomed in sample with different block sizes illustrated. The second figure illustrates the effect of the sizes on the results over the A1 dataset.

From the table above, we can notice that a larger size is undesirable as the feature mask is over sized resulting in a drop of accuracy.

Another hyper parameter to discuss is the number of scans/samples that will make one chunk of data, so instead of one image being passed individually, chunks of N images will make one "sample". In our case the chunks were decided at 10 samples, this is discussed previously, the authors of this work also chose to follow the same approach. The table below shows the impact of N over three architectures, at the largest value, the performances are close.

Training b-scans	$\mathcal{A}_1^{2D}$	$\mathcal{A}_2^{2D}$	$\mathcal{A}_3^{2D}$
$N = 1$	0.9468	0.9344	0.9247
$N = 3$	0.8956	0.9329	0.9195
$N = 5$	0.9320	0.9360	0.9230

Figure 45: Impact of N chunking over 3 similar CNN architectures.

Moving on we compare the results of their CNN architecture over their three 2-D datasets A1, A2 and A3 against our three, the MPG and Millbrooks pair. It is an observation that performances are reflected by the complexity of the architectures/techniques employed. However deeper classifier architectures will increase the rate of dimensionality reduction. Another thing to note is that feature extractors with higher overlap will increase the performance due to higher interdependency of adjacent samples.

As discussed previously, the 2-D results of the 3 CNN architectures will be compared with ours as a reasonable benchmark. We will only compare their results over Dataset S1 which was available online at github. The results over S2 were not verifiable as the implementation was not uploaded.
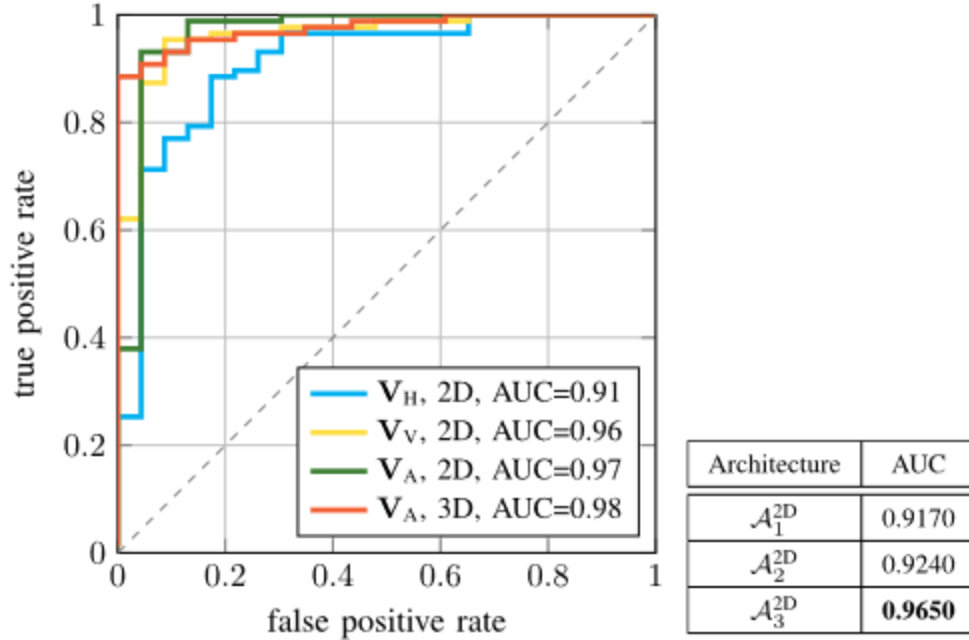
Figure 46: ROC curves of A3-2D over the dataset S1, the blue and yellow are results over horizontal/vertical polarization data. Green stands for A3-2D over the entire dataset and red is its 3d counterpart i.e. A3-3D over S1.

Features	MPGSept2005 (1791 samples)		
	SVM Linear	SVM-RBF	GRNN
HOG (8 bins)	93.23	72.29	87.09
LBP	72.29	NA	69.83
LBP (10 x 10 window)	77.97	72.29	75.52
ULBP (10 x 10 windows)	76.7	72.29	68.71
GRAB-ULBP (10x10 windows)	76.51	72.29	67.98
LESH	72.26	72.34	72.29
LPQ	82.64	72.29	72.29
WLD	60.22	72.29	64.19

Feature Extracting Technique	MPG2005Sep Net Avg Accuracy
HOG + LBP	78.31
HOG + LESH	93.22
HOG + LPQ + LESH	93.89
HOG + LPQ	93.95

Figure 47: Our empirical Results AUC (area under ROC curve) quoted in the tables.

As seen from the ROC comparison the discussed CNN architecture slightly beat us. Our best attempt HOG+ LPQ had an AUC of 93.95% against the A3-2D which had an AUC of 96.50%. This is a good performance when we observe that we are competing with CNN based architectures using implementations as simple as SVM and GRNN.
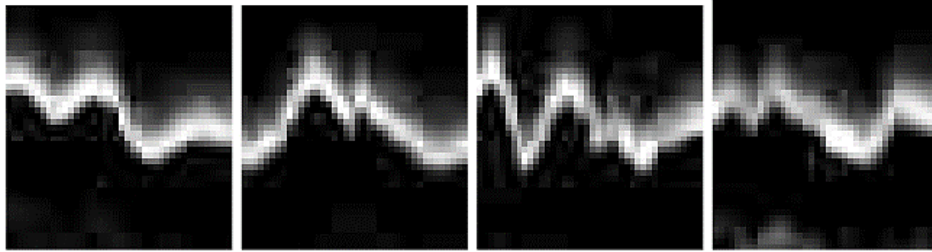
Classification Illustrated

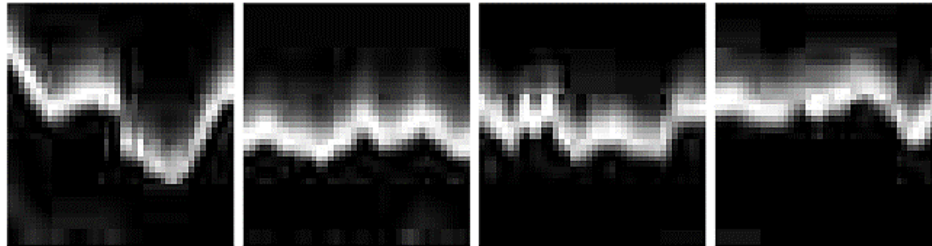Figure 48: Landmine Signatures correctly classified as Landmines.

Figure 49: Landmine Signatures misclassified as Clutter/Non-Mine Signatures
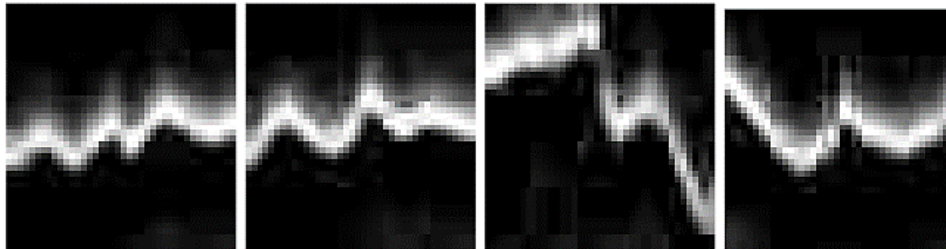

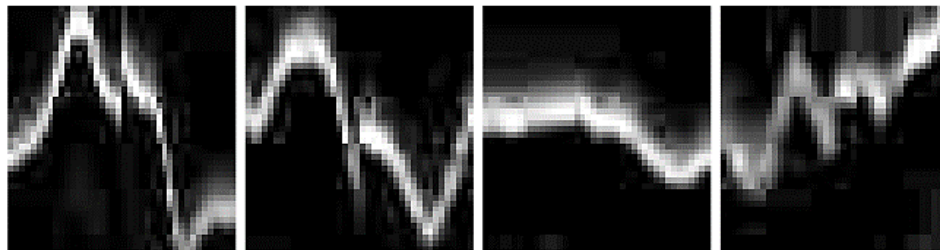Figure 50: Correctly Classified Clutter/Non-Mine Signatures

Figure 51: Non-Mine Signatures misclassified as Landmines.

4.6 Conclusion

Our main contribution in this thesis was to test and report the applicability of ESS or electromagnetic spectral signature based imaging techniques to detect and identify landmines in both surface deployment and buried deployment. As several regional conflicts continue to brew up such as Russia Ukraine war, Saudi Yemeni war, etc. the landmine crisis continues to grow across the world. There continues to be a need for fast and reliable solution based on whatever equipment is available as in many cases access to military grade detectors is not available either due to sanctions or political situations. Traditional techniques such as metal detector based listeners while being low cost are being phased out due to the nature of modern constructed landmines. Hyper spectral imagers are too expensive and not readily available in poor countries such as Pakistan, even less so are dedicated ground based radars or GPR. Small IR cameras are cheap and available thanks to the Chinese imports and can be mounted to a small drone to scan vast fields of land in a short period of time. It is further expected that the cost of both the portable cameras and drones will continue to fall as corporations will keep finding new technologies to enable cheaper mass manufacturing as demand increases.

For this project, we acquired data on electromagnetic spectral responses for American landmines primarily the claymore and the BLU-43 (butterfly) across various terrains and conditions. A spectral dictionary and bands were defined and the region around 750nm to 1100nm was selected which coincided with LWIR and MWIR bands. The datasets acquired had to undergo several pre-processing techniques and corrections. One major bottleneck over the signatures was background radiation or noise, which was primarily cause by solar energy. As we all know that the sun will not produce the same amount of energy/intensity for all bands/wavelengths, so the noise is random. There were also noise peaks at special intervals such as water absorption bands and CO_2 response bands. Another bottleneck we faced was that of buried landmines, on surface laid mines, we had distinct responses and discrimination was easy. In buried objects, we rely on signatures of camouflage material such as soil and grass. It will mostly depend on the amount of foliage over the mine.

In relative physics, every surface and material has its own electromagnetic signature according to which it reacts with spectral radiation such as light. This results in unique emittance and absorption responses and even color. By applying changing electromagnetic radiation over an object we can acquire an entire spectral curve which can then be used to decide if a certain object is present at a specific pixel location in the image. During our studies of the related pieces of literature, we observed the results of the previous tests such as the success of VNIR based imaging in detecting surface laid landmines. We also wrote a detailed theoretical explanation of why buried landmines change the thermal signatures of upper soil layers where they are buried and thus change in signature values of disturbed and un-disturbed soil and terrain can lead to detection of camouflaged landmines. The larger explosives are even easier to detect as their deployment will require digging up a greater area and disturb a larger amount of vegetation and soil. DRDC research across various bands reported that MWIR and LWIR are better performers at

buried object detection. We therefore decided to select a spectrum across a vast amount of bands and acquire real life datasets of images across them.

We rigorously tested all the processes involved from atmospheric corrections to classification, finding out how to reduce computation time to attain real time detection. There were several tradeoffs between detection performance and computing time. We studied several noise factors over the signatures such as wind and rain. In case of camouflaged landmines, rain decreases the amount of reflected thermal energy and thus reflectance response as water increased absorption. But the shape of the peaks and thus the overall signature remains intact. Thus more rain will result in the landmine's signature to overall be more similar to the foliage around it, making it harder to detect. Similarly using principle component analysis and other feature extractors do not always decrease computing time. We also concluded that the use of supervised detection is preferred as the False Alarm Rate is very much higher in unsupervised techniques as isolated signatures are reported while they are not landmines.

We then tested multiple architectures of supervised detection algorithms with our preference to use simpler lighter classifiers to keep computation cost and time minimal to the point that everything can be done in near real time on the lightest of computers, we thus avoided employing deep learning but we did include an entire section of performance comparison to CNN. In several scenarios we tested the performance of neural networks such as GRNN, others such as RBF and even linear SVMs, tabulating the results and reporting the entire performance curves. We concluded that several good candidate techniques could be used but proper pre-processing of training data and other parameters must be performed before deployment. In case of future works, focus should be given to optimize the project towards zero false alarm rates, more experimentation should be conducted in background noises and studying more terrains to test the classifiers more rigidly.

4.7   Future Work

There are several improvements that can be introduced, the first priority should be to acquire more datasets with similar settings to increase the amount of data available to the classifiers specially the GRNN and RBF Support Vector Machines as the current amount of data is low enough for Linear SVM to outperform them. In many Feature Extracting techniques, some system parameters such as number of bins in HOG, the normalization function, etc. should be changed and studied to improve performance. There should be more research on using key point Feature descriptors as that may lead to reduction of input feature dimensions.

The project can further be extended by removing some of our assumptions in the model. Until now the soil/terrain in the images was considered homogenous and considered a part of the background noise. The soil should be modelled mathematically and its inhomogeneous nature should be acknowledged, while this will introduce various minute and small anomalies which will

increase the FAR which we wished to minimized, this will make the project more robust. We can work towards arranging separate datasets for metal and plastic landmines and teach the algorithms to differentiate between the two. We can add more types of noise into the data to increase robustness other than just clutter and background radiation. These can include antenna cross talking a common phenomenon, air ground boundary bounce which happens when the signal first penetrates the ground. We can also add additive White Gaussian Noise or AWGN and finally we can add signal reflections. Signal Reflections are an interesting phenomenon to add as they depend on the material of the target and as such can lead to estimation of what kind of material the landmine is made from. Finally we can add further weather and real world conditions. The goal should be to work towards detection and classification with negligible error.

References

[1]   Landmine monitor report 2015 http://www.the-monitor.org/media/2152583/Landmine-Monitor-2015_finalpdf.pdf

[2]   M. Zucchetti, M. Khoder, I. Makki, R. Younes, C. Francis and T. Bianchi, "Landmines: Crisis, legacy, international and local action," 2017 First International Conference on Landmine: Detection, Clearance and Legislations (LDCL), Beirut, 2017, pp. 1-6.doi: 10.1109/LDCL.2017.7976954

[3]   Landmine Monitor Core Group," Towards a Mine Free World: Executive Summary", Feb 2016

[4]   UNICEF, "Children and Landmines: A Deadly Legacy", New York Sep 2013 https://www.unicef.org/french/protection/files/Landmines_Factsheet_04_LTR_HD.pdf

[5]   B. Ghali, "The landmine crisis: a humanitarian disaster. Foreign Affairs", Oct 1994 https://www.foreignaffairs.com/articles/1994-09-01/land-mine-crisis-humanitarian-disaster

[6]   Various, "Preface" in Landmine Monitor 2015, H. International, H. R. Watch, M. A. Canada, and N. P. s. Aid, ed Canada: International Campaign to Ban Landmines, 2015, p.iii.

[7]   N. Anderson, S. Paredes, "Social cost of land mines in four countries: Afghanistan, Bosnia, Cambodia, and Mozambique", British Medical Journal ,British Sep 2016

[8]   A.A. Berhe, "Landmines and land degradation: a regional political ecology perspective on the impacts of landmines on environment and development in the developing world." Michigan State University: East Lansing, MI (2000).

[9]   M.A. Buenker, "Landmines: A threat to wildlife and sustainability", World Conservation. 1: 19–20, Jan 200

[10]   International Campaign to Ban Landmines, "Landmine Monitor 2016 – Casualties &Victim Assistance," International Campaign to Ban Landmines Website. Available: http://www.the-monitor.org/en-gb/reports/2016/landmine-monitor-2016

[11]   International Campaign to Ban Landmines (September 2017), ICBL Website. Available: http://www.icbl.org/en-gb/the-treaty/treaty-in-detail/treaty-text.aspx

[12]   Global Security Fact Sheets, "Landmines", Jul 7, 2011

[13]   R.Keeley, "Understanding Landmines and Mine Action. MIT", Massachusetts Institute of Technology (US), Feb 2003

[14]   United Nations Mine Action Service (UNMAS), "Glossary of mine action terms, definitions and abbreviations ", New York Jan 2003

[15]   J. MacDonald, J.R. Lockwood, J. McFee, T. Altshuler, T. Broach, L. Carin,R. Harmon, C. Rappaport, W. Scott,R. Weaver," Alternatives for Landmine Detection", Pittsburg, RAND Science and Technology Policy Institute, Online book 2003, page:6-47

[16]   Dean, J. T. (Ed.), Project MIMEVA-Study of Generic Mine-like objects for R&D in Systems for Humanitarian Demining, Final Report, contract ref. AA 501852, European Commission, DG Joint Research Centre, Institute for System, Informatics and Safety, Technologies for Detection and Positioning Unit, Ispra, Italy, July 2001.

Available: https://www.gichd.org/fileadmin/pdf/LIMA/MIMEVA.pdf

[17]   Geneva International Centre for Humanitarian Demining, "Detectors and Personal Protective Equipment," Catalogue 2009.

[18]   M.G.Kale, V. R. Ratnaparkhe, A.S.Bhalchandra. "Sensors For Landmine Detection And Techniques: A Review", International Journal of Engineering Research & Technology (IJERT)Vol. 2 Issue 1, January- 2013 p:2-4.

[19]   C. P. Gooneratne, S. C. Mukhopahyay and G. Sen Gupta. "A Review of Sensing Technologies for Landmine Detection: Unmanned Vehicle Based Approach" , Institute of Information Sciences and Technology, Massey University, Palmerston North, New Zealand December 2004. P:401-407

[20]   M. Carrasco, D. Mery, L. Robledo. "A survey of land mine detection technology" International Journal of Remote Sensing Vol. 30, No. 9, 10 May 2009, p:2400-2404.

[21]   J. E. McFee ; K. L. Russell and M. R. Ito, "Detection of surface-laid minefields using a hierarchical image processing algorithm", Proc. SPIE 1567, Applications of Digital Image Processing XIV, 42 (December 1, 1991); doi:10.1117/12.50802

[22]   S. B. Achal ; J. E. McFee and C. D. Anger, "Identification of surface-laid mines by classification of compact airborne spectrographic imager (CASI) reflectance spectra", Proc. SPIE 2496, Detection Technologies for Mines and Mine like Targets, 324 (June 20, 1995);

[23]   J. E. McFee and H. T. Ripley, "Detection of buried land mines using a CASI hyper spectral imager", Proc. SPIE 3079, Detection and Remediation Technologies for Mines and Mine like Targets II, 738 (July 22, 1997)

[24]   T. Skauli, and I. Kåsen. "The effect of spatial resolution on hyper spectral target detection performance." In European Symposium on Optics and Photonics for Defence and Security, pp. 59870V-59870V. International Society for Optics and Photonics, 2005.

[25]   S. B. Achal; C. D. Anger; J. E. McFee and R. W. Herring "Detection of surface-laid mine fields in VNIR hyper spectral high-spatial-resolution data", Proc. SPIE 3710, Detection and Remediation Technologies for Mines and Mine like Targets IV, 808 (August 2, 1999)

[26]   T. Ivanco, S. B. Achal, C. D. Anger, and J. E. McFee, "Casi Real-Time Surface-Laid Mine Detection System", Proc. SPIE 4394, Detection and Remediation Technologies for Mines and Minelike Targets VI, 365 (October 18, 2001)

[27]   T. Ivanco, S. Achal, J. E. McFee, C. Anger, J. Young, "Real-time airborne hyper spectral imaging of landmines", Proc. SPIE 6553, Detection and Remediation Technologies for Mines and Minelike Targets XII, 655315 (April 26, 2007); doi:10.1117/12.720442

[28]   J. E. McFee, S. Achal, T. Ivanco and C. Anger, "A short wave infrared hyper spectral imager for landmine detection", Proc. SPIE 5794, Detection and Remediation Technologies for Mines and Mine like Targets X, 56 (July 08, 2005);

[29]   S. Achal, J. E. McFee, T. Ivanco and C. Anger, "A thermal infrared hyper spectral imager (tasi) for buried landmine detection", Proc. SPIE Conference on Detection and Remediation Technologies for Mines and Mine-like Targets XII, Vol. 6553, Orlando, FL, USA, 9-13 April, 2007, pp.655316-1-655316-11.

[30]   J. E. McFee, S. B. Achal, A. U. Diaz and A. A. Faust, "Comparison of broad-band and hyper spectral thermal infrared imaging of buried threat objects", Proc. SPIE Conference on Detection and Sensing of Mines, Explosive Objects and Obscured Targets XVIII, Volume 8709, Baltimore, MD, USA, 29 April - 03 May 2013.

[31]   J. E. McFee, A.A. Faust, Y.Das, K.L. Russell, "Final report Shield ARP 12 rl" – Optical imaging of explosive threats, August 2010.

[32]   A. A. Faust, J. E. Mcfee, R. H. Chesney, K. L. Russell, Y. Das, "Canadian Teleoperated landmine detection systems part I", International Journal Of Systems Science 36(9):511-528 · JULY 2005

[33]   J. E. McFee, K.L. Russell, R. H. Chesney, A. A. Faust, Y. Das, "The Canadian forces ILDS- A military fielded multi-sensor, vehicle mounted , teleoperated landmine detection system", Detection and Remediation Technologies for Mines and Minelike Targets XI, Proceeding of Spie (2006)

[34]   J. E. McFee ; C. Anger ; S. Achal and T. Ivanco, "Landmine detection using passive hyperspectral imaging", Proc. SPIE 6554, Chemical and Biological Sensing VIII, 655404 (April 26, 2007)

[35]   E.M. Winter, M. J. Schlangen, A.P. Bowman, M. R. Carter, C. L. Bennett, D. J. Fields, W. D. Aimonetti et al. "Experiments to support the development of techniques for hyperspectral mine detection." In Aerospace/Defense Sensing and Controls, pp. 139-148. International Society for Optics and Photonics, 1996.

[36]   A. P. Bowman, E. M. Winter, A. D. Stocker, and P. G. Lucey. "Hyperspectral infrared techniques for buried landmine detection." In Detection of Abandoned Land Mines, 1998. Second International Conference on the (Conf. Publ. No. 458), pp. 129-133. IET, 1998.

[37]   A. M. Smith, A.C. Kenton, R. Horvath, L. S. Nooden, J. Michael, J. A. Wright, J. L. Mars et al. "Hyperspectral mine detection phenomenology program." In AeroSense'99, pp. 819-829. International Society for Optics and Photonics, 1999.

[38]   A.C. Kenton, C. R. Schwartz, R. Horvath, J. N. Cederquist, L. S. Nooden, D. R. Twede, J. A. Nunez, J. A. Wright, J. W. Salisbury, and K. Montavon. "Detection of land mines with hyperspectral data." In AeroSense'99, pp. 917-928. International Society for Optics and Photonics, 1999.

[39]   M. T. Eismann, C. R. Schwartz, J. N. Cederquist, J.A. Hackwell, and R. J. Huppi."Comparison of infrared imaging hyperspectral sensors for military target detection applications." In SPIE's 1996 International Symposium on Optical Science, Engineering, and Instrumentation, pp. 91-101. International Society for Optics and Photonics, 1996.

[40]   L. B. Wolff ; D. A. Socolinsky ; C. K. Eveland ; J. I. Yalcin and J. H. Holloway, Jr. "Image fusion of shortwave infrared (SWIR) and visible for detection of mines, obstacles, and camouflage", Proc. SPIE 5089, Detection and Remediation Technologies for Mines and Minelike Targets VIII, 1298 (September 15, 2003).

[41]   E. M. Winter, M. A. Miller, C. G. Simi, A. B. Hill, T. J. Williams, D. Hampton, M. Wood, J. Zadnick, and M. D. Sviland. "Mine detection experiments using hyper spectral sensors." In Proceedings of SPIE, vol. 5415, pp. 1035-1041. 2004.

[42]   J.S. Groot, Y.H.L. Janssen, "Remote Land Mine (Field) Detection, an overview of techniques", TNO Physics and Electronics Laboratory, September 7, 1994.

[43]   N. Milisavljević and I. Bloch. "How can data fusion help humanitarian mine action?" International Journal of Image and Data Fusion 1, no. 2 (2010): 177-191.

[44]   N. Playle, "Detection of landmines using hyperspectral imaging." In Defense and Security Symposium, pp. 62170A-62170A. International Society for Optics and Photonics, 2006.

[45]   D. Letalick, I. Renhorn, O. Steinvall, "Multi-Optical Mine detection System (MOMS) final report", FOI Swedish Defence Research Agency, ISSN 1650-1942, December 2009

[46]   G. Suganthi, R. Korah, "Discrimination of Mine-Like Objects in Infrared Images Using Artificial Neural Network", Indian Journal Of Applied Research, Volume : 4 Issue : 12 , India, p 206-208, Dec 2014.

[47]   Thanh N.T., Hao D.N., Sahli H, "Infrared Thermography for Land Mine Detection in: Hammound R.I. (eds) Augmented Vision Perception in Infrared Advances in Pattern Recognition," Springer, London, 2009.

[48]   S. John, B. Eric, B. Koen, S. Klamer, T. Peter, B. Mario, F. Peter, C. Leo, M. Wannes and C. Richard, "LOTUS field demonstration of integrated multi-sensor mine-detection system in

Bosnia," Detection and Remediation Technologies for Mines and Minelike Targets VIII. SPIE Vol. 5089, 2003

[49]   "https://aviris.jpl.nasa.gov"

[50]   Coath, J.A.; Richardson, M.A. Regions of high contrast for the detection of scatterable land mines. In Proceedings of the Detection and Remediation Technologies for Mines and Minelike Targets V, Orlando, FL, USA, 24–28 April 2000; Volume 4038

[51]   Army Recognition. Army-2019: New UMZ-G Multipurpose Tracked Minelayer Vehicle Based on Tank Chassis.

[52]   Dolgov, R. Landmines in Russia and the former Soviet Union: A lethal epidemic. Med. Glob. Surviv. 2001

[53]   Maslen, S. Destruction of Anti-Personnel Mine Stockpiles: Mine Action: Lessons and Challenges; Geneva International Centre for Humanitarian Demining: Geneva, Switzerland, 2005

[54]   DeSmet, T.; Nikulin, A.; Frazer, W.; Baur, J.; Abramowitz, J.C.; Campos, G. Drones and "Butterflies": A low-cost UAV system for rapid detection and identification of unconventional minefields. J. CWD 2018

[55]   Pear, R. Mines Put Afghans in Peril on Return. New York Times. 1988. Available online: https://www.nytimes.com/1988/08/14/world/mines-put-afghans-in-peril-on-return.html

[56]   Dunn, J. Daily Mail. Pictured: The Harrowing Plight of Children Maimed in Afghanistan by the Thousands of Landmines Scattered Across the Country After Decades of War.

[57]   De Smet, T.; Nikulin, A. Catching "butterflies" in the morning: A new methodology for rapid detection of aerially deployed plastic land mines from UAVs. Lead. Edge 2018, 37, 367–371.

[58]   Baur, Jasper & Steinberg, Gabriel & Nikulin, Alex & Chiu, Kenneth & Smet, Timothy. (2020). Applying Deep Learning to Automate UAV-Based Detection of Scatterable Landmines. Remote Sensing. 12. 859. 10.3390/rs12050859.

[59]   Central Intelligence Agency. Afghanistan Land Use. The World Factbook. Available online: https://www.cia.gov/library/publications/resources/the-world-factbook/geos/af.html

[60]   F. Cremer, T. T. Nguyen, L. Yang, and H. Sahli, "Stand-off Thermal IR Minefield Survey: System concept and experimental results," Proceedings of SPIE, vol. 5794, pp. 209 – 220, 2005

[61]   F. Cremer, W. D. Jong, and K. Schutte, "Infrared polarization measurements of surface and buried anti-personnel landmines," In the proceedings of SPIE- Detection and Remediation Technologies for Mines and Minelike targets VI, vol. 4394, pp. 164-175, 2001

[62]   R. L. V. Dam, B. Boerchers, J. M. H. Hendrickx, and S. Hong, "Controlled field experiments of wind effects on thermal signatures of buried and surface-laid landmines"

[63]   F. Cremer, T. T. Nguyen, L. Yang, and H. Sahli, "Stand-off Thermal IR Minefield Survey: System concept and experimental results," Proceedings of SPIE, vol. 5794, pp. 209 – 220, 2005

[64]   J. Paik, C. P. Lee, and M. A. Abidi, "Image Processing-Based Mine Detection Techniques: A Review," Subsurface Sensing Technologies and Applications, vol. 3, pp. 153-201, 2002

[65]   C. T. Coutsomitros, A. Kokonozi, F. Andritsos, I. Vakalis, and L. v. Wijk, "Target identification in Humanitarian demining using weak activation IR methods," In the Proceedings of Euro conference- "Mine 99", Florence, Italy, pp. 131-136, 1999

[66]   P. Lopez, H. Sahli, and D. Cabello, "Detection and Classification of Landmines from Infrared Images," Removal and Neutralization of Landmines and UXO, 2003

[67]   V. A. Kotkar , S. S. Gharde, "Review Of Various Image Contrast Enhancement Techniques, International Journal of Innovative Research in Science, Engineering and Technology Vol. 2, Issue 7, July 2013.

[68]   C. P.Lee, "Mine detection techniques using multiple sensors." The Project in Lieu of Thesis, Electrical and Computer Engineering The University of Tennessee at Knoxville (2000).

[69]   Y. Wang, Q. Chen, and B. Zhang. "Image enhancement based on equal area dualistic sub-image histogram equalization method." IEEE Transactions on Consumer Electronics 45, no. 1 (1999): 68-75

[70]   J-M Gaucel, M. Guillaume and S. Bourennane. "Adaptive-3D-Wiener for hyperspectral image restoration: Influence on detection strategy." Signal Processing Conference, 2006 14th European. IEEE, 2006.

[71]   P.M. Mather and Magaly Koch. "Computer processing of remotely-sensed images: an introduction". John Wiley & Sons, 2011.

[72]   G. Noyel, J. Angulo, and D. Jeulin. "Morphological segmentation of hyperspectral images." Image Anal. Stereol 26, no. 3 (2007): 101-109.

[73]   L. Kaufman, and P. J. Rousseeuw. Finding groups in data: an introduction to cluster analysis. Vol. 344. John Wiley & Sons, 2009.

[74]   J. P. Benzecri, 1973." L'analyse de données 2, Dunod (1973).

[75]   C. Rodarmel and J. Shan. "Principal component analysis for hyperspectral image classification." Surveying and Land Information Science 62.2 (2002): 115.

[76]   Timo Ahonen, Abdenour Hadid, and Matti Pietikainen. Face description with local binary patterns: Application to face recognition. IEEE Trans. Pattern Anal. Mach. Intell., 28(12):2037–2041, December 2006

[77]   Archana Sapkota and Terrance E. Boult. Grab: generalized region assigned to binary. EURASIP Journal on Image and Video Processing, 2013(1):1–11, 2013.

[78]   N. Dalal and B. Triggs, "Histograms of oriented gradients for human detection," *2005 IEEE Computer Society Conference on Computer Vision and Pattern Recognition (CVPR'05)*, 2005, pp. 886-893 vol. 1, doi: 10.1109/CVPR.2005.177.

[79]   Summrina Kanwal Wajid and Amir Hussain. Local energy-based shape histogram feature extraction technique for breast cancer diagnosis. Expert Syst. Appl., 42(20):6990–6999, November 2015.

[80]   Zakir, U., Zafar, I., & Edirisinghe, A. E. (2011). Road sign detection and recognition by using local energy based shape histogram (LESH). International Journal of Image Processing, 4, 566–582

[81]   Esa Rahtu, Janne Heikkilä, Ville Ojansivu, Timo Ahonen, Local phase quantization for blur-insensitive image analysis, Image and Vision Computing, Volume 30, Issue 8, 2012, Pages 501-512.

[82]   Chen, Jie & Shan, Shiguang & Zhao, Guoying & Chen, Xilin & Gao, Wen & Pietikäinen, Matti. (2008). A robust descriptor based on Weber's Law. 10.1109/CVPR.2008.4587644.

[83]   R. Ablin, and C. H. Sulochana. "A survey of hyperspectral image classification in remote sensing." International Journal of Advanced Research in Computer and Communication Engineering 2.8 (2013): 2986-3000.

[84]   P.-N. Tan, M. Steinbach and V. Kumar, "Cluster Analysis: Basic Concepts and Algorithms", Chapter 8 in Introduction to Data Mining, Addison-Wesley, 2006, 487-567.

[85]   V. N. Vapnick, Statistical Learning Theory. John Wiley and Sons Inc.,1998

[86]   J. A. Gualtieri and R. F. Cromp, "Support vector machines for hyperspectral remote sensing classification," in Proceedings of the SPIE, vol.3584, 1999, pp. 221–232.].

[87]   G. Mercier and M. Lennon. "Support vector machines for hyperspectral image classification with spectral-based kernels." Geoscience and Remote Sensing Symposium, 2003. IGARSS'03. Proceedings. 2003 IEEE International. Vol. 1. IEEE, 2003.

[88]   C. M. Bishop, 1996, Neural Networks for Pattern Recognition. Oxford Univ. Press, Oxford

[89]   O. Laurino, R. D'Abrusco, G. Longo, G. Riccio; "Astroinformatics of galaxies and quasars: a new general method for photometric redshifts estimation", Monthly Notices of the Royal Astronomical Society, Volume 418, Issue 4, 21 December 2011, Pages 2165–2195

[90]   D. F. Specht, "A general regression neural network," in *IEEE Transactions on Neural Networks*, vol. 2, no. 6, pp. 568-576, Nov. 1991, doi: 10.1109/72.97934.

[91]   E. Parzen, "On estimation of a probability density function and mode," Ann. Math. Statist., vol. 33, pp. 1065-1076, 1962.

[92]   J . T. Tou and R. C. Gonzalez, Patrern Recognition Principles. Read-ing, MA: Addison-Wesley, 1974.

[93]   D. F. Specht, "Probabilistic neural networks," Neural Networks, vol.3, pp. 109-118, 1990.

[94]   D. F. Specht and P. D. Shapiro, "Training speed comparison of probabilistic neural networks with back-propagation networks," in Proc. Int. Neural Network Conf. (Paris, France), vol. 1 , pp. 440-443, July 1990.

[95]   D. F. Specht, "Probabilistic neural networks for classification, mapping, or associative memory," in Proc. IEEE Int. Conf. Neural Networks, vol. 1, pp. 525-532, June 1988

[96]   T. Poggio and F. Girosi, "A theory of networks for approximation and learning," A. I. Memo No. 1140. Artificial Intelligence Laboratory, Massachusetts Institute of Technology, July 1989

[97]   Bestagini, Paolo & Lombardi, Federico & Lualdi, Maurizio & Picetti, Francesco & Tubaro, Stefano. (2020). Landmine Detection Using Autoencoders on Multipolarization GPR Volumetric Data. IEEE Transactions on Geoscience and Remote Sensing. PP. 1-14.

[98]   I. Goodfellow, Y. Bengio, and A. Courville, Deep Learning. Cambridge, MA, USA: MIT Press, 2016.

[99]   H. Li and S. Misra, "Long short-term memory and variational autoencoder with convolutional neural networks for generating NMR T2 distributions," IEEE Geosci. Remote Sens. Lett., vol. 16, no. 2, pp. 192–195, Feb. 2019

[100]   H. Li and S. Misra, "Prediction of subsurface NMR T2 distributions in a shale petroleum system using variational autoencoder-based neural networks," IEEE Geosci. Remote Sens. Lett., vol. 14, no. 12, pp. 2395–2397, Dec. 2017.

[101]   R. Bello, "Literature review on landmines and detection methods," Frontiers Sci., vol. 3, no. 1, pp. 27–42, 2013.